Parametric Analysis for the Thermal Evaluation of Masonry Walls

by

Amy Huynh

A thesis submitted in partial fulfillment of the requirements for the degree of

Master of Science

in

Civil (Cross-disciplinary)

Department of Civil and Environmental Engineering

University of Alberta

Abstract

Newer energy codes for buildings in Canada now require energy losses associated with thermal bridging in smaller components to be accounted for. In masonry cavity wall systems, most of the energy losses from thermal bridging are due to structural penetrations at floor levels located at the shelf angles, the supports of the brick veneer. This is mostly due to shelf angles being designed following outdated guidelines, resulting in large steel shelf angles that creates bands of thermal leakage around the entire building. These old practices are gradually being replaced with intermittently spaced stand-off shelf angle connectors which reduce the cross-sectional area of thermal bridging. Another contributing factor of thermal bridging in shelf angle systems is that they are mostly made of steel, which is a highly conductive material. New technologies, such as plastic polymers, have been proposed to reduce thermal bridging losses, but there are few studies on the performance of the various types of polymers. The current industry standard of performance-based building code compliance is 3D numerical thermal modeling, which provides accurate predictions of the thermal performance of exterior building envelope systems. Although 3D numerical modeling is a highly reliable simulation method (if performed correctly), a limitation is the lack of capacity to run models at the level of complexity required by the building codes. It is also a costly and timely process because it is often contracted out to third party consultants.

This study uses 3D thermal modeling to investigate the influence of various parameters (i.e., stand-off shelf angle connector geometry, thermal properties, spacing of stand-off connectors, insulation thickness, and structural backup type) on the thermal performance of the envelope (i.e., heat flux through the assembly). These parameters were chosen as the focus of the study due to their high level of variability that may occur from detail to detail. A second goal

of this study is to use the results of the 3D models to determine a numerical relationship to calculate thermal bridging effects of various influential parameters, instead of having to model a new assembly each time.

For stand-off shelf angle connector geometry, it was found the heat flux difference between using a proprietary bracket and knife plate system was negligible. Additionally, reducing the spacing between stand-off shelf angle connectors appears to have the greatest range of influence on thermal performance for concrete masonry unit (CMU) backups on concrete slabs, and by extension, also steel stud backups. Wood stud backups are generally not affected by stand-off shelf angle connector spacing or insulation type and thickness. The linear transmittance results of the proprietary bracket, with a wood intermediate floor are almost the same value (same value when rounded to the nearest hundredth decimal point) regardless of insulation type and thickness. This is not surprising as the wood stud flooring has a low conductivity and the heat transferred from the interior to exterior that reaches the proprietary brackets is already a small amount. For CMU backups, changing from hot-dipped galvanized steel (HDG) steel to glass-fiber reinforced polymer (GFRP) knife plates, reduces the thermal bridging through the assembly because GFRP has a much lower conductivity than HDG steel. The difference appears to be more significant as the insulation thickness increases. For steel stud backups, the result from changing HDG to GFRP stand-off shelf angle connectors were more dramatic, as the GFRP connector had a linear transmittance that was nearly zero. This indicates that the full wall simulation provided a heat flux density value very close to its clear wall value. So generally, for a steel stud backup, a GFRP stand-off shelf angle connector is not considered a thermal bridge.

Preface

This thesis is an original work by Amy Huynh. Some of the research conducted for this thesis was submitted to the 14th Canadian Masonry Symposium conference, under "A Numerical Relationship for Effective R-Value Estimation of Shelf Angle Systems for Masonry Veneer".

Dedication

I would like to thank my supervisors, Yuxiang Chen and Carlos Cruz-Noguez for their continued kindness, support, and guidance throughout my research.

I would also like to thank Michael Hatzinikolas aka “Dr. Mike” for his mentorship and encouragement from the very beginning, and for always doubting my doubts.

And lastly, I would like to thank my family, my greatest gift, for their unconditional love and support.

Acknowledgments

I would also like to thank NSERC Engage Grants, Mitacs Accelerate program, and the Masonry Centre at the University of Alberta for funding this research.

Table of Contents

List of Tables

List of Figures

1 Introduction

The building sector accounts for 30 to 40% of world primary energy consumption and 20 to 30% of greenhouse gas (GHG) emissions. These values are expected to grow in the near future, given rising urbanization trends and building activity in developing countries (Dodoo, Gustavsson et al. 2011, Ibn-Mohammed, Greenough et al. 2013, International Panel on Climate Change 2014). It was reported by Natural Resources Canada that in 2018, 64% of secondary energy use was for space heating within the residential sector, and 60.5% within the commercial/ institutional sector, both taking the majority of shares by end-use (Natural Resources Canada 2018a, Natural Resources Canada 2018b). Many components and systems within a building contributes towards space heating. A vital component and a major influence for space heating is the building envelope, as it acts as the barrier between the interior and exterior environments and works against the energy impacts of the surroundings (Dimitrov 2015). A poor building envelope design can result in considerable energy consumption and rapid degradation of the structure. Improper detailing contributes to high thermal conduction, air leakage, and moisture condensation in the walls that can lead to damage. With aims to reduce the environmental impacts of building energy consumption and to boost energy performance, governments and third-party organizations have implemented more restrictive energy codes and other voluntary green building rating tools (GBRTs). A common approach in improving building energy efficiency is to increase the R-value of exterior walls, which was shown of importance in the latest versions of the National Energy Building Code of Canada for Buildings (NECB) and ASHRAE Standard 90.1 (National Research Council of Canada 2017, ASHRAE 2019). These standards provide detailed information for the appropriate U and R-Values of building elements

such as walls, roofs, and floors. Increasing the R-Value of these building elements reduces the amount of heat loss that is experienced, especially with cold exterior temperatures.

1.1 ***Heat transfer fundamentals***

The mechanisms of heat transfer that are considered when evaluating a building envelope involve conduction, convection, and radiation. They are categorized based on the interaction between the subatomic particles and their macro movements. Particle collision takes place within conduction and convection, whereas macro movements occur within radiation. Conduction accounts for the building envelope materials that are in direct contact with each other (not including air). The basic equation for conduction under a steady state analysis is given by Fourier's law, is described in Equation (1) below.

$$q = A\frac{k}{l}(t_1 - t_2) \tag{1}$$

where

q is the rate of heat flow in units W/m^2;

A is the area perpendicular to the direction of heat flow in m^2;

k is the coefficient of thermal conductivity in W/mK;

l is the length of flow path or thickness of the material; and

t_1 and t_2 are the temperatures at either end of the flow path so $(t_1 - t_2)$ is the temperature difference.

Convection involves the movement of fluids, such as air, and can take place between a solid and a fluid. Radiation involves the exchange of heat through electromagnetic waves and

does not require a medium to occur (i.e. can occur in a vacuum). Within a building envelope, convection and radiation occurs on the exposed inner and outer-most layers because of the air near the surfaces. Combined coefficients for radiative and conductive-convective exchanges are given in the ASHRAE Fundamentals handbook. These values are affected by many factors and can be chosen based on various parameters such as surface emissivity and direction of heat flow.

1.2 ***Thermal Bridging***

Thermal bridging is a popular buzzword when it comes to energy performance, as it is a result of a highly conductive penetration through the building envelope where major heat losses occur. By simply increasing insulation thickness without accounting for thermal bridging will reduce the effectiveness of the insulation, and increase the overall cost of the project (Alhawari and Mukhopadhyaya 2018). Some examples of major thermal bridging areas include cantilevered balconies and exposed slab edges, and if neglected, can result in the underestimation of 20 to 70% of the total heat flow through walls (Alhawari and Mukhopadhyaya 2018, Morrison Hershfield Limited 2019, Morrison Hershfield Limited 2020). It is difficult to specify the weight of thermal bridges, which can vary from 5% (retrofitting the exterior of the building envelope) to 39% (in heavily insulated single-family homes with a large thermal bridge) (Martin, Erkoreka et al. 2010). The weight can depend on several factors such as the insulation thickness, material type, weather conditions, building use, or even how the weight is calculated.

With respect to masonry wall systems, one of the most significant areas of thermal bridging occurs at almost every floor level - traditional steel shelf angles, which are often used on multi-storey residential, commercial, and institutional buildings to support full-bed masonry veneers. Figure 1 describes the general components of a masonry wall cavity.

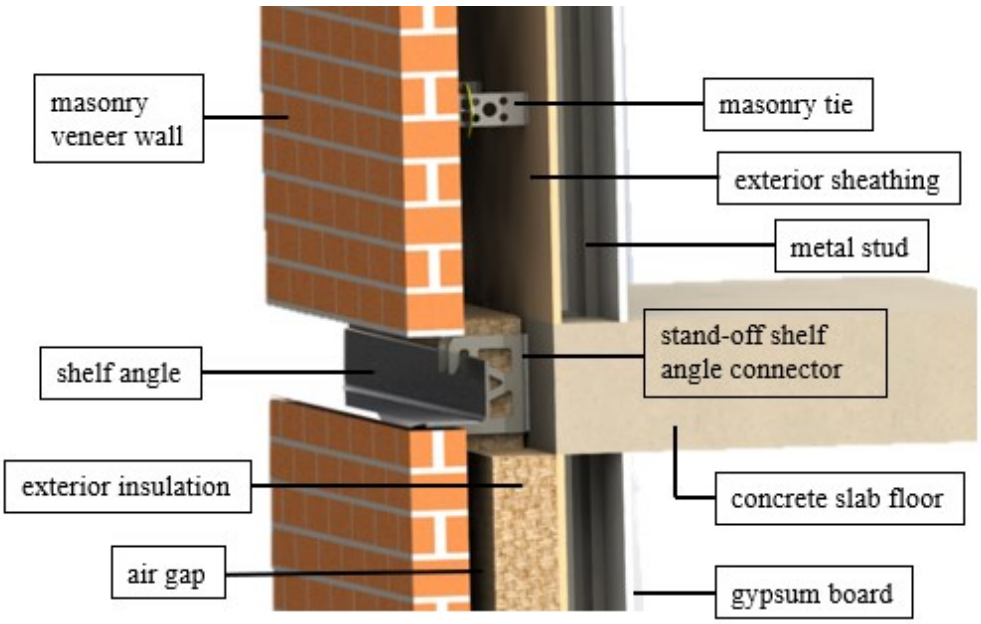

Figure 1. Metal stud backup, wall cavity detail

It has been found that shelf angles are a significant thermal bridge that can reduce the effectiveness of insulation by 50% or more (Finch, Wilson et al. 2013). Findings such as these, relating to the significance of thermal bridging, have influenced energy codes such as the National Energy Code of Canada for Buildings (NECB) to change. Since transitioning from NECB 2011 to NECB 2017, more stringent requirements for calculating the overall thermal transmittance of the building assembly have been implemented. NECB 2011 allows neglecting major structural elements and other elements that completely penetrate the building envelope as long as the sum of the cross-sectional areas were less than 2% of the above-ground building envelope area (National Research Council of Canada 2011). This 2% allowance was removed in NECB 2017 to improve the overall thermal performance of buildings in Canada and must now be accounted for in an analysis of the thermal transmittance of a building's envelope (National Research Council of Canada 2017). This is a significant change for masonry veneer systems because it requires that both masonry ties and masonry shelf angles that were typically exempt

from thermal bridging calculations in NECB 2011, must be now accounted for in the calculation of overall thermal transmittance.

1.3 ***Code Compliance for Thermal Bridging***

The performance path for energy code compliance as outlined by NECB is typically favored among designers as it offers the most flexibility. NECB 2017 lists the Building Envelope Thermal Bridging Guide (BETB) by Morrison Hershfield Limited and BC Hydro as an acceptable resource to use in performance path thermal bridging calculations. The guide provides thermal bridging values of various building assemblies so the user does not have to perform complicated 3D computer simulations themselves. In Appendix A of the BETB, assembly details are presented, including dimensions, a list of assembly components, conductivity, density, and specific heat values. Figure 12 in **Appendix A, Section A.1 Additional Figures** shows an excerpt from Appendix A of the BETB.

Once the user has located the detail of interest to their project, the detail # located at the top left corner and may be referenced to Appendix B of the BETB, which contains the thermal modeling results. See Figure 13 in **Appendix A, Section A.1 Additional Figures** for an example. The model results are presented as an R and U value, with a calculated linear transmittance if applicable. R-Values are used to define the level of thermal resistance in units of m^2K/W. R-Values can be applied to single components or an entire system. The higher the R-Value, the more thermally resistant a component or system is. The U-Value is the reciprocal of an R-Value so it has units of W/m^2K and defines the level of thermal transmittance of a component or system. Conversely, the higher the U-Value, the less thermally resistant a component or system is (or alternatively, it can transmit more heat).

The method described in the BETB allows designers to use the given R, U, and linear transmittance values in their project without having to perform 3D simulations themselves. Due to current modeling technologies available, avoiding 3D simulations provides greater access to energy-efficient designs because more options can be presented in an efficient manner. It also further simplifies the thermal bridging calculation process, and reduces the time and cost of the design phase. By making the calculations less complicated, it will feel less like a chore for designers and can help promote a more positive attitude towards more energy efficient building envelope designs. Avoiding complicated methods and calculations for thermal bridging is ideal, and a main goal of this research. The motivation for this research stems from a reaction to the recent change in building codes, now requiring thermal bridging calculations, and an industry need to further simplify and provide greater access to thermal masonry wall details for designers, architects, engineers, building envelope consultants, and more.

1.4 ***Research Purpose***

A building envelope has many components that can affect the heat flow through the assembly, and creating a new model or simulation for a single parameter change can be time consuming and costly. This paper presents 3D thermal computer simulations with a focus on varying parameters such as insulation thickness, stand-off shelf angle connector configuration (proprietary bracket and traditional knife plates), stand-off material (Hot-Dipped Galvanized (HDG) Steel and Glass Fibre Reinforced Polymer (GFRP)), stand-off spacing (1220 mm and 610 mm), and structural backups (concrete masonry unit, wood stud, and steel stud) to establish a numerical relationship (i.e. numerical multiplier) that accounts for these various parameters to capture a range of scenarios, rather than presenting a single value or a single scenario. This study was conducted using a 3D finite element modeling software, ANSYS, to produce a thermal

simulation database for masonry wall assemblies. The results from the simulations helped to determine multipliers that can be applied to wall assemblies when calculating thermal bridging effects. The multipliers can be applied to current models in the BETB guide, and/ or to new models proposed in this paper, that has the ability to account for additional or changing parameters, thus maximizing the utility of these thermal models. The multiplier can also be generally applied to account for scenarios beyond what was modelled in the database and the intermediate cases (e.g., thermal insulation between selected values). This parameter multiplier method provides a step towards further simplifying the thermal evaluation of masonry shelf angle supports for exterior-insulated walls. The purpose of this research can be summarized into 3 parts:

1. To provide a parametric analysis to determine how certain parameters and components affects the heat flux through the masonry assemblies. Parameters such as insulation thickness, material type, geometries, and structural backup types; and

2. To provide an alternative multiplier method in determining the thermal bridging effects of masonry shelf angles on various types of masonry wall assemblies, with the intent of providing results in a timely manner and for general precision to be used during the design phase of a project; and

3. To provide accurate, precise heat flux and linear transmittance results of some masonry veneer wall assemblies that are absent from the BETB. These results may be used independently or in conjunction with the BETB.

*1.5 **Organization of Thesis***

This thesis is organized into 6 sections:

Section 1, Introduction describes the background of thermal bridging and its significance to masonry building envelope systems. The motivation for this research stems as a reaction to the recent change in building codes, now requiring thermal bridging calculations, and an industry need to further simplify and provide greater access to thermal masonry wall details. The purpose of this research is to provide an alternative method in determining the thermal bridging effects of masonry shelf angles (with the intent of general precision to be used during the design phase of a project); to provide a parametric analysis using various parameters that affects the heat flux moving through the assembly; and to provide precise heat flux and linear transmittance results of masonry veneer wall simulations.

Section 2, Literature Review addresses the thermal bridging effects of masonry shelf angles and its influence on building codes based on published research. The literature review covers topics such as thermal bridging effects and energy consumption, best practices in improving the energy efficiency of building envelopes, previous studies on the thermal performance of shelf angles using both 2D and 3D methods, past and recent methods used to calculate and measure thermal bridging, NECB 2017 requirements relating to thermal bridging, and the BETB.

Section 3, Methodology describes the finite element analysis modeling methodology used in this research, including the thoughts and development of the modeling assumptions. It is broken down into Sections *3.1, 3.1.1 Physical and Model Assembly Geometry, 3.1.2 Validation ,* and *3.2 Data Analysis.* Section *3.1.1* describes the full assembly and individual component

geometry (with figures) and material conductivities (shown as either standard or calculated values). Section 3.1.1 breaks down the boundary conditions, contact resistances, and mesh of the finite element models. Section 3.1.2 describes the validation process of the model, with an explanation of reasoning and assumptions. Section *3.2* explains the parameters chosen for the models and reasoning for it, and the multipliers are introduced.

Section 4, Results and Discussion presents the results of the simulations in tabular form. The results are separated by backup type: CMU, wood stud backup, steel stud backup, and a section for cross-backup relationships. For each backup type, simulation results are presented as values of heat flux density and linear transmittance, and multipliers are calculated and shown for various scenarios. The discussion for each backup type follows the results in the same section. The discussion compares the thermal differences when manipulating the various parameters and presents relationships drawn from the results.

Section 5, Conclusion summarizes key findings and conclusions of this study, taken from the results and discussion. *Section 5.1* discusses the limitations of the study and *Section 5.2* discusses future research recommendations.

2 Literature Review

Buildings consume approximately 40%, 25%, and 40% of the world's energy, water and resources, respectively, and are responsible for emitting a third of total greenhouse gas (GHG) emissions (Ruparathna, Hewage et al. 2016). Energy use forecasts show that future energy consumption in commercial buildings are expected to increase whereas decrease in residential buildings (United States Department of Energy 2012, Ruparathna, Hewage et al. 2016). Thus, improving building energy efficiency, especially in commercial buildings, is a critical step towards reducing the overall environmental effects due to our energy consumption. Structural design and energy efficiency were once thought of as separate responsibilities. It was intended for structural engineers to take on the weight of designing a system to provide for the structural integrity of the building and for others such as architects, mechanical engineers, and building envelope consultants to handle the energy efficiency portion (Anderson, D'aloisio et al. 2012). This is no longer the case as greater efforts to improve overall building energy efficiency are being implemented. Areas that were traditionally not taken into consideration, such as structural members, are now being challenged. It has taken some time for the construction industry to acknowledge research evidence for significant thermal losses due to highly conductive structural members penetrating the building envelope and insulation (i.e. thermal bridging), but fortunately governmental bodies are actively including thermal bridging to be accounted for in building codes.

2.1 ***Thermal Bridging Effects***

Minimizing thermal bridging and increasing the effective resistance values is listed as a best practice approach in a guide listed by The Government of Newfoundland and Labrador (The Government of Newfoundland and Labrador 2016). In regards to thermal bridging, a study in

2012 (Anderson, D'aloisio et al. 2012) concluded that up to 4% in annual energy savings could be achieved if thermal bridging was accounted for in the masonry building design using the 2D heat transfer program THERM; this article provided a model building that accounted for thermal bridging details such as rooftop grillage posts, roof edge angles, shelf angle supports, masonry lintels, and cantilever roof canopy beams. Improving heat transfer models (e.g. using 3D instead of 2D) can further save energy because systems can be integrated, further refined, and optimized together. On a separate occasion, HEAT3 was used to evaluate the thermal performance of masonry systems (Finch, Wilson et al. 2013). The analysis showed that directly anchored shelf angles reduced the effectiveness of the exterior insulation R-Value by 40 to 55%, making it difficult to attain necessary R-Values required for code-compliance. More recently in 2019, a similar finding was presented by A. D. Placido, B. Brown, D. Chong, and C. Schumacher (Placido, Brown et al. 2019), who found that shelf angles can reduce the effectiveness of the exterior insulation by 50%. In comparison, they found that using intermittent connectors, spaced according to specifications, which would improve insulation continuity throughout the building, reduces the effectiveness of the R-Value by only 15%. As a result of findings such as these, the latest version of the NECB (2017) now accounts for thermal bridging in structural members requires that all structural penetrations, including those with areas less than 2% (which was allowed by previous versions of the code to be neglected), must now be accounted for in calculating the effective thermal resistance of a building's envelope (National Research Council of Canada 2017).

An additional trend is that many proprietary systems are now offered on the market to bridge structural design with energy efficiency, providing further support to mitigate thermal bridging issues. Many companies offer systems that provide the structural design as either included in the

cost or their testing data is publicly available, which is prescriptive in nature given pre-engineering. Some of these systems use special materials that have low thermal conductivities such as Glass Fibre Reinforced Polymer (GFRP) or with patented cross-sectional shapes that reduces the contact area between conductive elements and the exterior insulation (thus reducing the amount of heat flow) without compromising the structural integrity of the component.

2.2 ***Thermal Bridging Calculation Methods***

Methods to calculate thermal bridging have evolved quickly over-time. A methodology proposed by Hassid, was based on an integral approach on 2D equations that accounted for thermal bridging effects across multilayer walls, presented as an approximate analytical expression (Hassid 1990). The wall types included were homogenous, insulation outside the main wall, insulation in the middle of the main wall, and insulation inside the main wall. Another methodology calculated thermal bridge effects by using a quantitative analysis based on thermographic surveys (Asdrubali, Baldinelli et al. 2011). The air temperature was measured using infrared thermography, in which the thermal bridging effect was estimated as a percentage of the total wall thermal transmittance. The incidence factor of the thermal bridge was introduced in this paper, defined as the ratio between the heat flowing in real conditions and the heat flowing in absence of the thermal bridge. A method more applicable to building energy simulation (BES), was based on the equivalent wall method: in which a thermal bridge that is typically represented in 2D or 3D, is replaced with an equivalent 1D multilayer wall (Quinten and Feldheim 2015). This is desirable in BES programs (such as EnergyPlus or TRNSYS) because they generally use 1D heat transfer equations. A similar and more recent study by Kim and Yeo aimed to develop a thermal bridge modeling and dynamic analysis method to be integrated into 1D BES programs (Kim and Yeo 2020). It was justified in the paper that thermal

bridging requires 3D modeling to account for its complexities, and in order to be used in a BES program, the thermal bridge must be converted into a simpler 1D analysis. A clear wall is analyzed in the study and the thermal bridge is assumed to be a linear time-invariant system, modeled using a data-driven method. The thermal bridge model was also proposed in a dynamic analysis method to calculate the heat flow.

2.3 ***Thermal Bridging and Building Codes***

The current industry standard to calculating thermal bridging is based in 3D model simulations, and is heavily referenced to in the NECB. NECB 2017 offers three paths of compliance: prescriptive, trade-off, and performance. In regards to thermal transmittance, the prescriptive path presents minimum RSI values with respect to the building envelope, that must be met. The trade-off path offers some flexibility in design for the above-ground assemblies, given that the calculated overall transmittance of the proposed building is not more than the overall transmittance of the reference building. The performance path offers the most flexibility in design, provided that the simulated energy consumption of the proposed building is equal to or less than the reference building, whose performance is based upon the prescriptive requirements of the code (National Research Council of Canada 2017). The performance path is typically favored among designers as it offers the most flexibility. Hand calculations for R-Value estimation are often used and most material conductivities and surface resistances for air films were taken from Section 26 of the 2009 ASHRAE Handbook Fundamentals, but this simplified 1D method is difficult to account for the thermal bridging of the entire assembly (Love and Klee). In order to account for the diverse and sometimes proprietary technologies available, as well as the complexity of large wall assemblies, 3D computer simulations are required. Simple hand calculations or 2D models are mostly insufficient for this level of complexity. 2D models

can only present linear thermal bridging or details at certain cut sections of the wall assembly, which may be useful for specific details, but to provide enough information on the full effect of the thermal bridge, a 3D model is necessary to comply with building code requirements. The level of accuracy of linear transmittance calculations also differs depending on the method type. ISO 14683 presented that numerical calculations have a typical accuracy of ± 5%, thermal bridge catalogues as ± 20%, manual calculations as ± 20%, and default values ranging from accuracy 0 to 50% (International Organization for Standardization 2017).

2.4 ***Thermal Bridging Guides***

The downside of 3D computer simulations is that it can be time consuming and the software required can be costly. At times, the contractor is delegated the task of providing the thermal detail and the process may be difficult as this is a relatively new concept and what is needed by the code is often debatable. The number of models, the level of detail of each model, and how many variations to include for assurance, are a few questions that could take weeks to negotiate and decide on, which also differs per project. This work is then sought out from 3rd party companies, where only a few have the capacity to run these simulations. Some rates currently start at $5000 for the first model, and $500 for any additional ones. In efforts to address the cost and time management aspect of thermal modeling, and to make the comprehensive thermal bridging modelling more accessible, Morrison Hershfield Limited and BC Hydro released the BETB. The BETB's target audience are architects, engineers, and other building design professionals, with the intent of showing how to recognize and mitigate thermal bridging impacts. The guide is essentially a database that provides building envelope details to account for the impact of thermal bridging of various assemblies, which include both generic and proprietary systems. The guide presents a list of building assemblies that addresses many current

needs for thermal bridging calculations. The guide utilizes clear wall and interface details, described as opaque building components. A clear wall assembly includes all of the general components of a wall assembly that may contain thermal bridges from small uniformly distributed elements such as masonry ties or steel studs. An interface detail is an assembly that "…changes in construction or geometry that interrupt the uniformity of the clear field [clear wall]" ; this includes slab edges, opaque to glazing wall transitions, parapets, corners and through wall penetrations (Morrison Hershfield Limited 2020). The difference between the heat flow through an interface detail and a clear wall assembly detail, would result in the additional heat flow due to the thermal bridge, which could either be represented as a linear or point transmittance. Linear transmittances are dependent only on the linear length (or width) of the assembly and is represented with a ψ in units of W/mK. Linear transmittances are not included in the clear wall assemblies and typically occur at interface details (Morrison Hershfield Limited 2020). An example of a linear transmittance would be a masonry shelf angle. A point transmittance is a single point of additional heat flow (i.e. not dependent on area or length) and is represented with a χ in units of W/K. Point thermal bridges are also not included in clear wall assemblies. An example of a point transmittance would be a structural beam penetration through the exterior insulation, with the structural beam perpendicular to the face of the exterior insulation (Morrison Hershfield Limited 2020).

$$U_T = \frac{\sum(\psi * L) + \sum \chi}{A_T} + U_o \tag{2}$$

where

U_T is the total effective assembly thermal transmittance in W/m^{2}K;

ψ is the linear transmittance in W/mK;

L is the length of the thermal bridge in m;

χ is the point transmittance in W/K;

A_T is the total area of the opaque wall area in m^2; and

U_o is the clear field thermal transmittance.

The BETB details are broken into an "Appendix A – catalogue material data sheets"; and "Appendix B – catalogue thermal data sheets". Appendix A describes the various assemblies fully in detail with labels, specifying material thickness, conductivity, resistance, density, and specific heat of each component. Appendix B provides the R-values, U-Values, clear wall values, linear and point transmittance values of each assembly. Although thermal bridge catalogues provide a comprehensive list for their thermal bridging calculations which utilizes plug and play values, a complete list for all scenarios is naturally unattainable. There are an endless amount of possible combinations and scenarios that makes this a difficult and impractical long-term solution.

3 Methodology

A finite element analysis software, ANSYS Workbench was utilized to calculate the heat flux values of various masonry assemblies. The assemblies consisted of CMU, wood stud, and metal stud wall backups, which were first constructed in SolidWorks before being imported into ANSYS. The simulation data were verified by comparing with simulations performed by others which had identical geometries. Then the results were used to calculate the linear transmittances and to conduct a parametric analysis of the assemblies. Upon collecting all of the thermal data from the completed simulations, numerical multipliers were calculated to be used in heat flux/ linear transmittance estimations during the design phase of a project.

The thermal simulation results are presented as a heat flux density (W/m^2) (also known as heat flux or thermal flux). This value represents the heat that is passing through the assembly per square meter. This value is then converted into a U-value (W/m^2K) by dividing by the temperature difference applied to the assembly, and may be used to calculate the linear transmittance (W/mK) of the assembly. The U-Value may be converted into an R- or RSI-Value (thermal resistance value) by taking the inverse of it. Numerical multipliers were presented for both heat flux and linear transmittance results (i.e., the multipliers may be applied to model results shown in units W/m^2 for heat flux or W/mK for linear transmittance). The data may be used in collaboration with the calculation methods outlined in the BETB, as means to maximize practitioner use. A limitation of this study was that the simulations were not validated against real experiments as planned, due to lab closures regarding COVID-19.

3.1 Model Development

3D models of various building envelope assemblies were simulated under steady-state thermal analysis conditions using the commercially available finite element analysis ANSYS software. It is a comprehensive finite element modeling package with various types of analysis systems such as structural, hydrodynamic, fluid flow, electric, and thermal. The assemblies focus on masonry wall veneers with various backup types such as CMU, wood stud, and steel stud.

A clear wall (or clear field) assembly model removes major structural penetrations such as shelf angles and balcony slabs but includes elements like masonry ties, along with the other basic components like insulation, backup/ framing, and exterior materials. With respect to the models in this study, the main difference between the full wall assemblies and clear wall assemblies is that the concrete slab or wood flooring, shelf angle, and shelf-angle offset connectors are removed in the clear wall assemblies. The number of wall assemblies for each wall back up type is described in Table 1, below. The full wall assembly is one with all components (including structural penetrations) included.

Table 1. Number of assemblies for each wall backup

Wall Backup Type	Number of Full Wall Assemblies	Number of Clear Wall Assemblies
CMU	20	4
Wood Stud	8	4
Steel Stud	9	3

3.1.1 Physical and Model Assembly Geometry

The wall backup of a building is designed to resist loads such as dead, live, wind, and seismic movements. It is rare for reinforced brick masonry to function as a structural backup

type (Mason Contractors Association of America 2021). The assemblies modeled in this study consists of three structural backup types: concrete masonry/ concrete block, wood stud, and steel stud. The exterior of all assemblies is brick masonry veneer. In this case, the exterior (unreinforced) masonry veneer is not a structural component of the wall structure, it is to provide protection for the interior building envelope from the outdoor elements only. The following paragraphs will provide brief descriptions of the general building envelope components and the different backup types.

In all models, a 10 mm thick exterior and interior film was applied to the surfaces of the outermost or innermost components (i.e., the masonry veneer wall, gypsum board, and flooring) to account for the air near the surfaces that experience convective and radiative heat transfer. Those combined heat transfer coefficients can be applied directly in the model as a layer of thermal resistance. A 25 mm air gap was also accounted for in all assemblies, placed directly behind the masonry veneer. The masonry veneer consists of standard brick with 10 mm mortar beds between each course, placed in a running bond pattern. Proprietary face mounted masonry ties with an L-shaped plate (Figure 2) were included in the models. The L-plate plate is mounted to the face of the backup (or exterior sheathing, depending on the type) and spans across the insulation and air space, with a V-shaped wire attached to the other end of the L-Plate that becomes embedded in the mortar during the brick laying process. The masonry tie used in these models also have holes punched through the L-Plate that aims to reduce the amount of steel-to-insulation contact and cross-sectional area parallel to the wall surface (thus reducing the amount of thermal bridging), without compromising its structural integrity. The depth (projection of the tie parallel to the wall surface) and thickness of the plate varies depending on the insulation thickness. For thicker insulation sizes that are 152.4 mm and above, the thickness changes from

1.6 mm to 3.18 mm. See Figure 2 for masonry tie details. The lemon-shaped component that lies perpendicular to the depth of the tie is made of polyethylene and its function is to help prevent the insulation from detaching from the backup. The rest of the tie is made from hot dipped galvanized (HDG) steel.

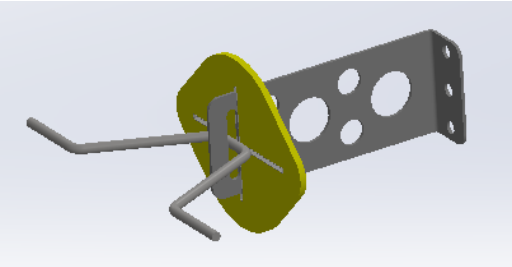

Figure 2. Masonry tie

(size for 101.6 mm of insulation shown)

The shelf angles (Figure 1) used in all cases were 6.35 mm thick and have 101.6 mm equally long flanges. This shelf angle size is commonly used with the proprietary bracket, as it is typically stocked product among steel suppliers, thus readily available at a low cost. Two different types of stand-off shelf angle supports (e.g., herein "stand-off") were used in the model simulations. One is a proprietary product that utilizes a C-shaped bracket (see Figure 3) made of HDG steel, with holes cut out from the body similar to the masonry ties. The shelf angle is mechanically fastened to the bracket by first slipping the angle into the top flanges and then laying it down across the bottom flange (see Figure 1 for details). The second type is a traditional knife plate assembly (see Figure 4). It is composed of a backer plate (parallel to the face of the wall) typically welded to a knife edge (protrudes perpendicular to the face of the wall). Then the knife edge is then welded to the angle for connection. The knife plates were made with either HDG steel or Glass Fiber Reinforced Polymer (GFRP) materials. Note that the

knife plate geometry in this study is a generic detail that may not be structurally sufficient (especially for the thicker insulation sizes) and was constructed for the sake of thermal comparison only. The connector depth for both systems varied depending on the insulation thickness. The depth is referred to as the projection of the bracket or knife plate parallel to the surface of the wall.

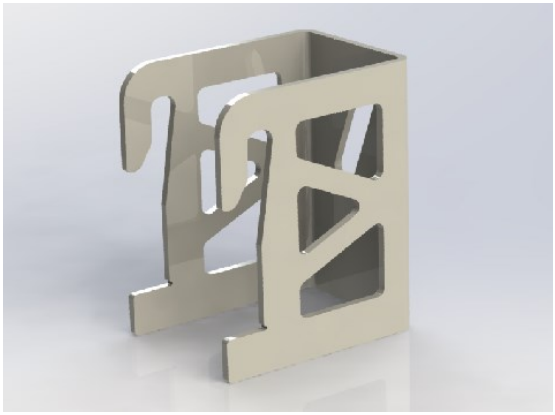

Figure 3. Proprietary shelf angle support bracket
(size for 101.6 mm of insulation shown)

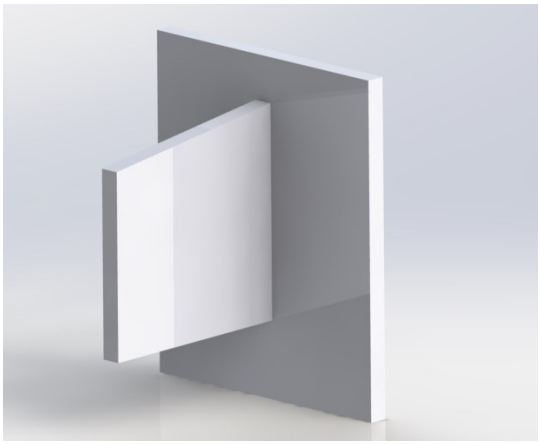

Figure 4. Generic welded knife plate for shelf angle support
(size for 101.6 mm of insulation shown)

The **concrete masonry backup** assemblies were geometrically based on two-cell, size 20 block with an actual width, length and height of 190 mm x 390 mm x 190 mm, medium weight concrete block units (CMU), with 10 mm of mortar applied between each CMU. For structural considerations, typically every fourth cell is fully grouted, and the remaining cells not grouted. To simplify the block geometry for 3D modeling, the grouted blocks, un-grouted blocks, and the mortar were represented by fully solid rectangular prisms. Since every fourth cell was considered fully grouted, an entire column of the wall was modeled as one solid rectangular prism (dimensions: 190 mm width, 1210 mm height, and 200 mm length which includes both the block and mortar) separating two other solid rectangular prisms (dimensions: width, height and length of 190 mm x 1210 mm x 600 mm and 190 mm x 1210 mm x 400 mm, respectively) representing the un-grouted cells. Each rectangular prism was given different equivalent thermal conductivities. The entire width of the wall is 1200 mm which is based on the typical spacing of the stand-offs. This is further illustrated in Figure 5.

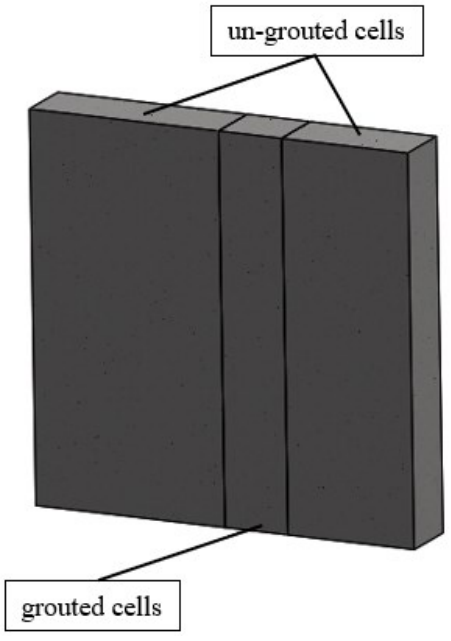

Figure 5. Simplified CMU backup geometry, Configuration 1

The rectangular prism is near the center is the column of grouted cells. An alternative, Configuration 2, of grouted and un-grouted CMU was also modeled to see the effect of two grouted columns. Configuration 2 relied on starting with a grouted core column of cores, followed by three columns of un-grouted cells, another column of grouted cells, and finally one last column of un-grouted cells.

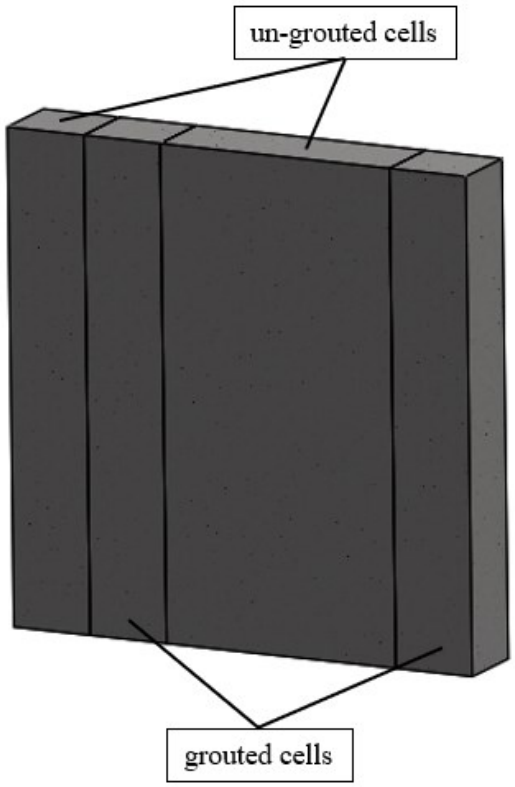

Figure 6. Simplified CMU backup geometry, Configuration 2

This configuration is similar to the last in that every fourth cell is still fully grouted but it presents 2 fully grouted cores in the assembly instead of one. Because of this, the heat flux density is expected to be slightly higher as the un-grouted cells with still air within has a lower conductivity than the grouted cells. Upon modeling, the difference between the 2 models was less than 0.5%, so Configuration 1 was maintained for the remaining CMU assemblies.

The assembly accounts for a CMU wall that extends 1210 mm high in each direction, with a 203 mm intermediate concrete slab floor, as shown in Figure 7. The exterior insulation for the concrete masonry backup assemblies ranges from 101.6 mm (4 inches) to 254 mm (10 inches) of mineral wool insulation. The exterior insulation is placed in direct contact and is continuous with the backup system and intermediate floor (to avoid any floor edge losses during simulation). These variables are further discussed in **Section *3.2, Data Analysis.*** Furthermore, 41 mm steel studs were placed towards the interior of the concrete masonry wall, spaced at 406 mm on center to support an interior gypsum board layer.

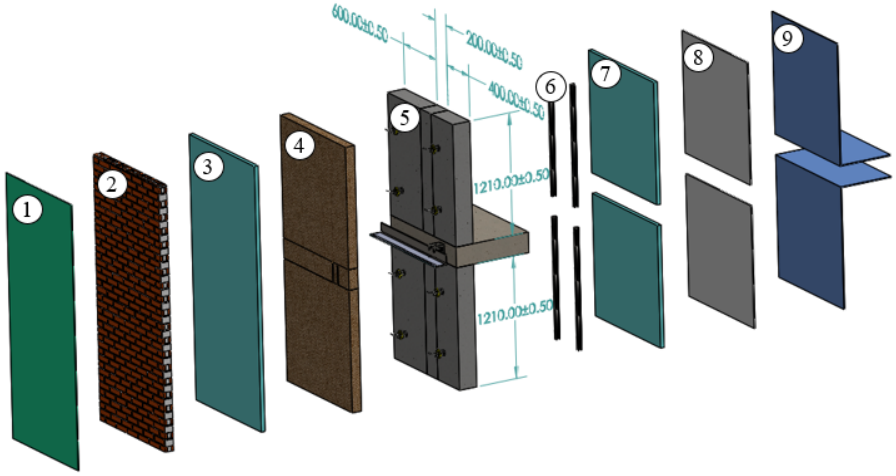

Component #	Component(s)
1	Exterior film
2	Masonry veneer
3	Air space
4	Insulation
5	CMU, masonry ties, shelf angle, shelf angle support, concrete slab
6	Steel studs
7	Air between steel studs
8	Gypsum board
9	Interior Film

Figure 7. Concrete masonry backup

(shown with concrete slab flooring, units in mm)

The **wood stud backup** assemblies were built with 38 mm x 140 mm wood studs, spaced 406 mm on center, and filled with 140 mm thick fiberglass batt insulation between the studs. See Figure 8.

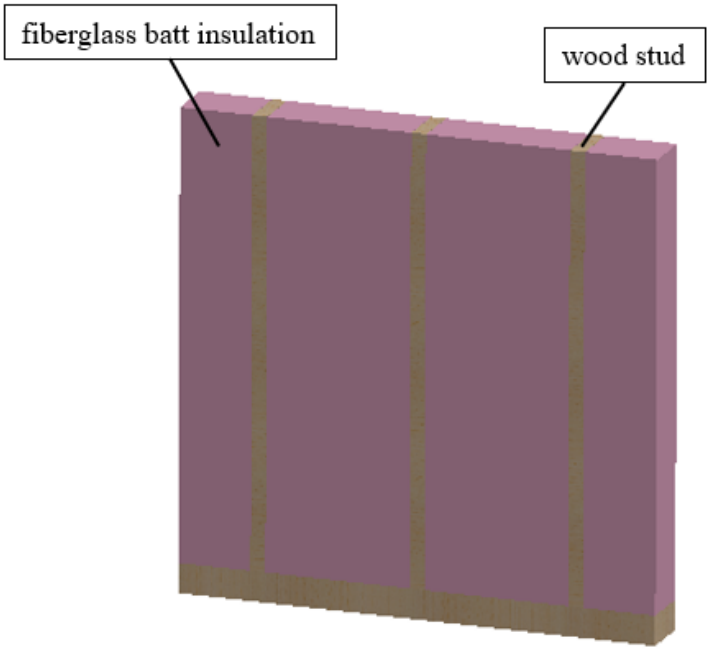

Figure 8. Wood stud backup geometry

A gypsum board layer is placed towards the interior of the wall, with a plywood sheathing placed on the exterior of the fiberglass batt insulation. The exterior insulation varies between 50.8 mm and 101.6 mm of extruded polystyrene insulation (XPS) and mineral wool insulation, respectively. Two types of flooring have been constructed for the wood stud backup: (1) a 38 mm x 235 mm wood rim joist with wood joists, including wood flooring and fiberglass batt insulation at the joists, and (2) an intermediate concrete slab as seen in the concrete masonry backup (Figure 7). Two other conductivity variations were modelled for the intermediate concrete slab. The conductivities modeled were 10 times (18 W/mK) and a tenth (0.18 W/mK) of the original intermediate concrete slab (1.8 W/mK). These values were chosen to examine the

influence of the floor conductivity on the thermal response of the wall systems.

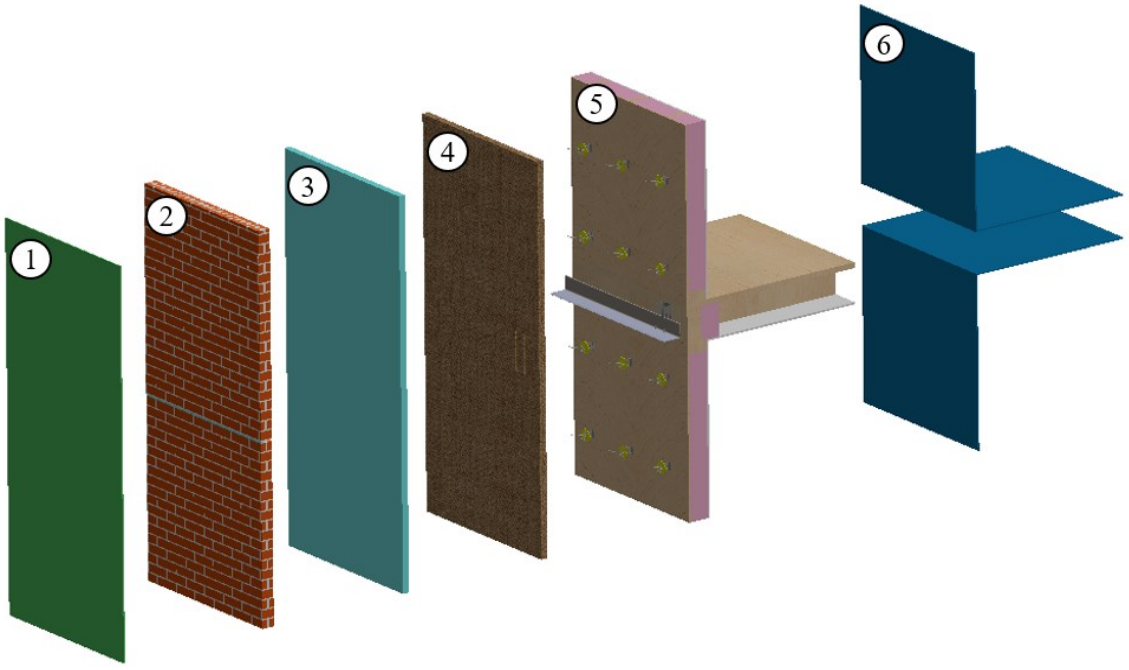

Component #	Component(s)
1	Exterior film
2	Masonry veneer
3	Air space
4	Insulation
5	Exterior plywood sheathing, wood stud, fiberglass batt insulation, rim joist, wood flooring, gypsum board, masonry ties, shelf angle, shelf angle support
6	Interior film

Figure 9. Wood stud backup (shown with wood rim joist and wood joist flooring)

The **steel stud backup** assemblies were constructed with 92 mm x 41 mm, 0.9 mm (20-gauge) steel studs with top and bottom tracks. The studs were spaced at 406 mm on center and were not filled with any insulation between, only air. The exterior insulation is mineral wool and ranges from 101.6 mm to 203.2 mm. This is a smaller insulation thickness range than the CMU wall backups because 203.2 mm is typically the upper limit of what is usually specified. The

limit was pushed to 254 mm for CMU to determine potential relationships with a larger data set. Gypsum board was placed towards the interior side of the stud and a layer of exterior sheathing on the other side.

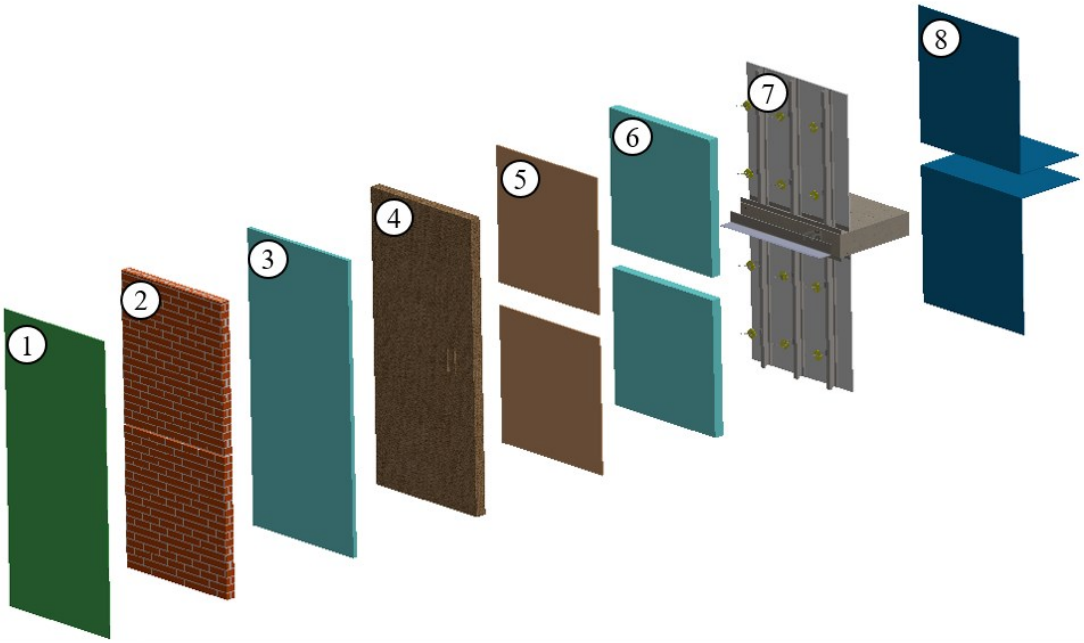

Component #	Component(s)
1	Exterior film
2	Masonry veneer
3	Air space
4	Insulation
5	Exterior plywood sheathing
6	Air between steel studs
7	Steel studs, concrete slab, gypsum board, masonry ties, shelf angle, shelf angle support
8	Interior film

Figure 10. Steel stud backup

(shown with concrete slab flooring)

Table 2 summarizes the geometry of the wall components and backup system. The conductivity of each component is also given. These values were taken from the 2009 ASHRAE Handbook (American Society of Heating Refrigerating and Air-Conditioning Engineers 2009) and the BETB so that the findings in this paper may be used in collaboration with the methods in the BETB and building code.

Table 2. Wall components: dimensions and conductivity

Component	**Dimensions (mm)**	**Conductivity (W/mK)**
Interior Film[2]	10 thick	0.083
Gypsum Board	23 thick	0.16
Air in Stud Cavity	92 thick	0.57531
Un-grouted Concrete Block	190 x 390 x 190	0.87[1]
Grouted Concrete Block	190 x 390 x 190	1.13[1]
Wood Stud	38 x 140	0.1
Steel Stud	92 x 41, 0.9 thick	62
Fiberglass Batt Insulation	140 (just for wood stud)	0.042
Exterior Mineral Wool Insulation	50.8 to 254 (varies)	0.034
Extruded Polystyrene Insulation	50.8 and 101.6	0.029
Face-Mounted Masonry Ties (Hot-Dip Galvanized)	1.6 thick 3.175 thick	62
Intermediate Concrete Slab	203 thick	0.8, 1.8, 18
Proprietary Bracket	4.76 thick	50
Knife Plate	4.19 backer plate 9.53 knife edge	50 for galvanized steel
	4.19 backer plate 12.7 knife edge	0.2 for GFRP
Shelf Angle	101.6 x 101.6, 6.35 thick	50
Vented Air Cavity	25 thick	0.3571
Brick	190 x 57, 90 thick	0.78
Brick Mortar	10 thick	0.5
Exterior Film[2]	10 thick	0.34

[1] Calculated values (see below).
[2] Interior and exterior films are needed in order to apply the convective and radiative heat transfer coefficients experienced by the air near the surfaces. It is applied as a layer of thermal resistance.

The equivalent thermal conductivity value for the un-grouted concrete blocks was taken as an approximation from the 2017 ASHRAE Fundamentals handbook (American Society of Heating Refrigerating and Air-Conditioning Engineers 2017) and the Metric Technical Manual

from the Canadian Concrete Masonry Producers' Association (Canadian Concrete Masonry Producers' Association). The equivalent thermal conductivity for a fully grouted block was calculated using values from the ASHRAE Fundamentals handbook and a series-parallel (also known as isothermal planes) R-Value calculation.

The GFRP material conductivity was chosen as 0.2 W/mK. This was an assumption taken from a study that found that GFRP's thermal conductivity using a steady-state measurement method was 0.1534 W/mK and using a transient method was 0.3228 W/mK (Fernandes 2014). Additionally, a similar proprietary thermoset resin in the BETB has a thermal conductivity of 0.2 W/mK. Table 3 presents the full assembly dimensions.

The vented air cavity conductivity was taken from the BETB. Codes such as ISO 6946 and ASHRAE 2017 defines values for air cavities but they are un-ventilated values. The one provided by the BETB is a ventilated value, therefore has a higher conductivity and is more realistic than the un-ventilated values due to the presence of weep holes in masonry veneers.

Table 3. Assembly dimensions

	CMU Backup	Wood Stud Backup	Steel Stud Backup
Overall Height (mm)	2623	2712	2642
Overall Length (mm)	1200	1219	1219
Concrete Slab Projection[1] (mm)	800	800	800
Rim joist, wood flooring Projection[1] (mm)	N/A	1333	N/A

[1] Perpendicular to the face of the veneer wall, towards the building interior.

Boundary Conditions:

The interior and exterior temperatures used in the boundary conditions of all the simulations were 21°C and -18°C, respectively, as detailed in section 3.1.1.5. of NECB 2017 and ASTM C 1363 (International 2011, National Research Council of Canada 2017). These boundary temperatures are applied to create a temperature difference across the assembly so that the overall heat flux of the assembly can be calculated. These temperatures were applied to the exterior faces of the interior and exterior films (see *Section 3.1.1* and Table 1 for more details). Convective and radiative boundary conditions are accounted for as a layer of resistance via the interior and exterior films. Adiabatic boundaries were accounted for on the side faces of the assembly (i.e. the remaining exposed faces in the two other directions where the interior and exterior temperatures were not applied).

Contact Resistances:

The contact resistances between materials were taken from ASHRAE 1365-RP. It should be noted that ASHRAE 1365-RP mentions that the contact resistance between studs and the sheathing in steel-stud backups appear to be the most important factor to predict the overall thermal resistance of an assembly. Otherwise, the heat flux will be over-predicted (i.e. the total heat flux from the model will be higher than the actual) by up to a 10% difference between tested and simulated results (Desjarlais and McGowan 1997, Patrick Roppel 2011). This is also re-iterated by the 2009 ASHRAE Handbook where it states that the contact resistances in building are too small to be of concern in many cases, but might be important for steel framing due to its high conductivity. The contact resistances from ASHRAE 1365-RP are summarized in Table 4 below.

Table 4. Contact resistances from ASHRAE 1365-RP

Assembly Location	Contact Resistance ($m^2°C/W$)
Steel flanges at sheathing interfaces	0.030
Insulation interfaces	0.057
Steel to concrete interfaces	0.057
Steel to steel interfaces	0.011

For the models used in this study, it was ensured that the steel flanges and sheathing interfaces were given the correct contact resistance. The remaining contact resistances from Table 4 were also applied, but not to every single component. This is because the contact points of some components are very small (e.g. masonry ties: V-Tie to L-Plate contact) in comparison to the whole model and would not make a significant difference to the total heat flux of the model. This is also re-iterated by 2009 ASHRAE Handbook where it states that the contact resistances in building are too small to be of concern in many cases, but might be important for steel framing due to its high conductivity. This was coupled with the information given by ASHRAE 1365-RP in which the contact resistance of the steel stud to sheathing is most important, to rationalize omitting the contact resistance of smaller components that would lower the efficiency of creating these models. In any case, a fully bonded (i.e. providing no contact resistance between materials) contact provides a more conservative value in the end. Table 5 below summarizes the components considered when applying the contact resistances from Table 4. It can be assumed that any other components not specified in the table below were given fully bonded contacts during the simulations.

Table 5. Contact resistances applied to models

Assembly Location	Backup	Components accounted for
Steel flanges at sheathing interfaces	CMU	Steel flange to interior CMU face
	Steel Stud	Steel flange to exterior plywood sheathing
	Wood Stud	N/A
Insulation interfaces	CMU	Insulation to exterior CMU face, insulation to backside of shelf angle, insulation to shelf angle supports
	Steel Stud	Insulation to exterior plywood sheathing, insulation to backside of shelf angle, insulation to shelf angle supports
	Wood Stud	
Steel to concrete interfaces	CMU	Steel stud to concrete slab, shelf angle support to concrete slab
	Steel Stud	
	Wood Stud	Shelf angle support to concrete slab
Steel to steel interfaces	CMU	Shelf angle support to shelf angle
	Steel Stud	
	Wood Stud	

Mesh:

The element size used for a majority of the elements was 2 mm. This was a value that allowed for an accuracy for which the solution output (total heat flux applied at the exterior face of the exterior film) converged at a reasonable value. A small element size value was especially required for the thinner geometry components such as the masonry ties and steel studs. For

example, the wood stud back up with proprietary brackets, 50.8 mm of XPS insulation, and wood intermediate floor, the heat flux value for the 2 mm mesh is 7.78 W/m^2. The 4 mm and 6 mm mesh give similar values. Therefore the 2 mm mesh presents a more reasonable value. The ANSYS Workbench advanced sizing feature was applied to the radial or non-square elements such as the mortar, brick, and shelf angle supports. The mesh that is automatically created is generally finer than the 2 mm at these locations, see Figure 11 below.

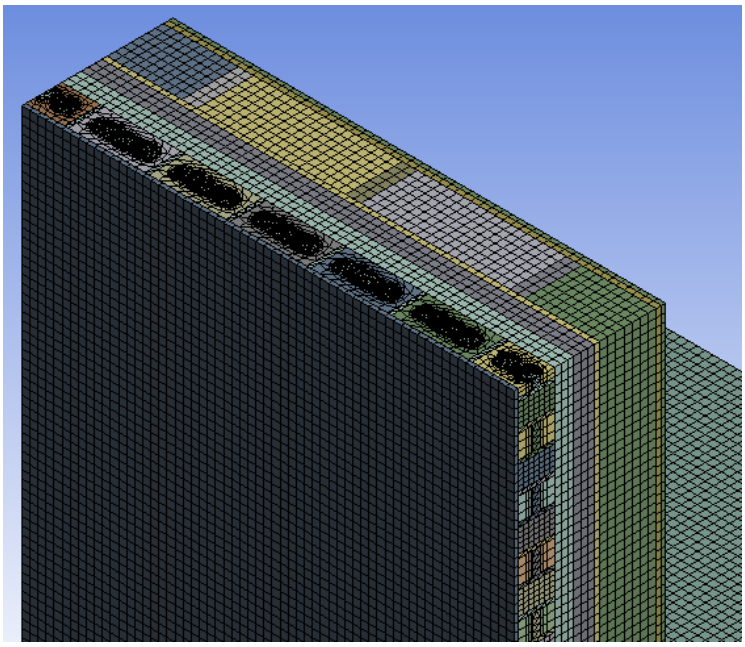

Figure 11. Isometric view of a wood stud assembly mesh (zoomed in for detail)

3.1.2 Validation

The first step of building the masonry assemblies was to geometrically replicate one of the models provided in the BETB. Additionally, the modeling methods used in the BETB was the same as ASHRAE 1365-RP. The models in ASHRAE 1365-RP were compared to guarded hot-box data sets (29 assemblies) to demonstrate that their models can accurately reproduce results similar to measured tests. The goal of this research validation was to create a

model such that the overall U- or R-value would be within 10% of the one provided in the BETB to ensure a reasonable level of conformity and agreement. The validation model was based on Detail 5.2.33, Scenario 2 (See Figure 12 and Figure 13 in **Appendix A, Section A.1**) with an exterior insulation 1D R-Value of 16.8 of the BETB. A majority of the dimensions and conductivity values are taken from the BETB as described in Table 1 and Table 2. Although the modeling programs between the BETB and this paper differ, it was expected that the final results are similar as the same thermal fundamentals were applied. The 3D finite element analysis program used by the Thermal Bridging Guide is a heat transfer software package by Siemens PLM Software; FEMAP and Nx, with Maya's TMG thermal solver (Patrick Roppel 2011). The simulations indicated the overall U- or R-Value of the validation model was within 10% of the geometrical twin provided in the BETB. The results were achieved by setting the interior temperature and exterior temperature as per NECB 2017 guidelines and as per ASHRAE 1365-RP. The difference between the U-Values of the clear wall and full wall assemblies between the BETB assembly and the assemblies of this thesis were 5.3% and 8.9%, respectively. This provided confidence in creating the remaining models with a similar method.

As an additional validation, another researcher within our lab independently simulated 4 CMU backup assemblies to compare the values against. The same methodology was adhered to, but the difference was that some contact resistances were neglected. The only contact resistance accounted for in this set of simulations, were the steel flanges at the sheathing interfaces (See *Section 3.1.2* for more details on contact resistances). The backup in these simulation cases were CMU so the difference is even further minimized (i.e. not steel stud backup), and a fully bonded contact was applied to the other areas. So, in any case, a fully bonded (i.e., providing no contact resistance between materials) contact provides a more conservative value (i.e., smaller R and

higher heat flux) in the end. Results showed negligible differences from 5.51 to 9.24% between the models developed in this second study and the previous models. These validation models were also built directly in the ANSYS SpaceClaim program instead of being imported from SolidWorks, which may have contributed to the differences.

3.2 Data Analysis

The parameters chosen for this research were based on common variations that are found in masonry building envelope assemblies. The first parameter considered was insulation thickness as it can fluctuate greatly from project to project. Accounting for different insulation thicknesses is crucial when adhering to a performance-based energy compliance method as other factors such as the total window area or HVAC system efficiency can influence the required thickness (among other factors) to comply with codes. Stand-off shelf angle connector configuration is often varied as well. Two common but different systems were considered in the simulations: a proprietary bracket system and generic welded knife plates, with the latter usually designed by structural engineers thus varying in dimensions from project to project. See *Section 3.1.1*, Figure 3 and Figure 4 for further details on the stand-off shelf angle connectors. In terms of thermal bridging, GFRP materials (and other similar plastics) are becoming more popular due to its low thermal conductivity so this was an additional material variation applied to the knife plates to compare its thermal performance to traditional HDG steel. The stand-off shelf angle connector spacing is also an essential parameter to consider as there may be many variations to consider based on the project details. And finally, all of these parameters were applied to three different structural backup types: CMU, wood stud, and steel stud. See *Section 3.1.1, Physical and Model Assembly Geometry* for further details on the structural backup systems. These 5 parameters were chosen as the independent variables in order to find the influence of the heat

flux through the assembly, or the linear transmittance/ thermal bridging (the dependent variable). It is assumed that no other components or materials were changed between models of the same backup type other than the 5 independent variables. The parameters are summarized in the table below.

Table 6. Parameters varied in this study

Parameters varied in this study	**Value Range/ System Types**
Insulation thickness	101.6 mm to 254 mm (4" to 10"), in 50.8 mm (2") increments
Stand-off shelf angle connector configuration	Proprietary bracket or knife plates
Material	HDG steel or GFRP
Stand-off shelf angle connector spacing	1220 mm (4') or 610 mm (2')
Backup Type	CMU or wood stud or steel stud

A parametric analysis will be further discussed in parallel in **Section 4 Results and Discussion**. From the data compiled during the parametric analysis, heat flow trends through the assembly are analyzed based on changing the insulation thickness; stand-off connector type, material, spacing; backup system; intermittent slab type. The parametric analysis is conducted based on the heat flux density and linear transmittance values of the assembly. The formulation and calculation of the linear transmittance is presented below.

Calculation of Linear Transmittance:

A linear thermal transmittance value, ψ (W/mK) is be presented in **Section 4**, **Results and Discussion** for each of the models. One of the numerical outputs from an ANSYS thermal model is average heat flux density, q (W/m^2), for the entire exterior face of a wall assembly. This value is then used to calculate linear thermal transmittance value, ψ (W/mK), using Equations (3) to (6):

Use ANSYS output q (W/m^2) to calculate thermal transmittance per unit area, u (W/m^{2}K):

$$u = \frac{q}{\Delta T} \tag{3}$$

where

ΔT is the temperature difference applied to the assembly (39 K in this case).

And to calculate the thermal transmittance of a given area, U (W/K):

$$U = u \cdot Area_{wall} \tag{4}$$

where

$Area_{wall}$ is the area of the exterior wall, taken as the product of the overall height and overall length of the wall as defined in Table 3.

To find the ψ (W/mK) value of the full wall assemblies, the thermal transmittance of the clear wall assemblies must be incorporated into the calculation (American Society of Heating Refrigerating and Air-Conditioning Engineers 2017, Morrison Hershfield Limited 2020) . A clear wall assembly model removes major structural penetrations like a shelf angle but includes elements like masonry ties along with the other basic components like insulation, backup/ framing, exterior materials. With respect to the models in this study, the main difference between the clear wall assemblies and full wall assemblies is that the concrete slab, shelf angle, and shelf-angle offset connectors are removed in the clear wall assembly.

$$\psi_{full\ wall} = \frac{U_{full\ wall} - U_{clear\ wall}}{L_{wall}} \tag{5}$$

where

$U_{full\ wall}$ is the thermal transmittance of the full wall assemblies, calculated using Equations (3) and (4), above;

$U_{clear\ wall}$ is the thermal transmittance of the clear wall assembly, also calculated using Equations (3) and (4), but with a different q;

and L_{wall} is the overall length of the wall as defined in Table 3.

Alternatively,

$$\Psi_{\text{full wall}} = \frac{U_{\text{full wall}} - U_{\text{clear wall}}}{L_{\text{wall}}} = \frac{u_{\text{full wall}} \cdot \text{Area}_{\text{wall}} - u_{\text{clear wall}} \cdot \text{Area}_{\text{wall}}}{L_{\text{wall}}}$$

$$= \frac{(u_{\text{full wall}} - u_{\text{clear wall}}) \cdot \text{Area}_{\text{wall}}}{L_{\text{wall}}} = \frac{\left(\frac{q_{\text{full wall}}}{\Delta T} - \frac{q_{\text{clear wall}}}{\Delta T}\right) \cdot \text{Area}_{\text{wall}}}{L_{\text{wall}}}$$

$$= (q_{\text{full wall}} - q_{\text{clear wall}}) \frac{\text{Area}_{\text{wall}}}{\Delta T \cdot L_{\text{wall}}} = (q_{\text{full wall}} - q_{\text{clear wall}}) \frac{h_{\text{wall}}}{\Delta T}$$

An example calculation is provided in **Appendix A, Section A.2** using the data presented in **Section 4, Results and Discussion**.

Calculation of Multipliers:

To establish a numerical relationship between the various scenarios, multiplicative factors, or multipliers, were given to each model solution. The multipliers were determined using Equation (5)

$$M_i = \frac{q_i}{q_{i-1}} \tag{6}$$

where M_i is the multiplier of the current scenario;

q_i is the simulation result of the current scenario under analysis (W/m^2);

and q_{i-1} is the simulation result of the previous scenario under analysis (W/m^2).

Two types of multipliers are presented in **Section 4, Results and Discussion**: one is based on the heat flux density solution and the other is based on the calculated linear transmittance of the assembly. They are named "multipliers" because they are meant to be multiplied against a given heat flux density or linear transmittance value. The multiplier is chosen based on a parameter (or a set of parameters) that the user chooses, and applied to an assembly with a given/ existing heat flux or linear transmittance value. The multiplier then changes the given/ existing value into an assembly that accounts for the chosen parameter. For example, if the heat flux density of a steel stud backup with 4" of insulation and HDG knife plates was known, but a project required 6" of insulation with GFRP knife plates, a multiplier to account for the increase in insulation and a multiplier for changing from HDG to GFRP knife plates could be applied to solve for the unknown heat flux of the project. This is an example with 2 parameters.

Equations (3) and (4) define how heat flux density q (W/m^2) is converted to thermal transmittance per unit area (u, W/m^2K) and of a given area (U, W/K). The multiplier for q is thus extended to both u and U as they are directly proportional to each other. This can be further extended to other similar terms such as R-Value and RSI, in which the thermal transmittance of the assembly would be divided by the multiplier (instead of being multiplied) since R-value is the inverse of thermal transmittance.

The purpose of the multiplier is to provide a numerical relationship that can account for the heat flow difference when changing parameters such as insulation thickness, thus eliminating

the need to run a completely new simulation if that is the only change (e.g. insulation thickness) in an existing model. In some cases, the heat flux or linear transmittance isn't provided for intermediate cases or other varying parameters in a thermal bridging guide, as providing a model for every scenario is practically impossible. The multiplier provides an alternative method to obtain a reasonable heat flux or linear transmittance value of an assembly in a timely manner.

4 Results and Discussion

The results in this section presents the data of the parametric analysis (values of heat flux density and linear transmittance) and calculated multipliers. Each are separated by backup type. Following the tabled numerical results for each backup type is a discussion for each parameter type.

4.1 ***CMU Backup***

Table 7 displays the heat flux density, q (W/m^2) results of the ANSYS simulations (see *Section 3.1.1 Physical and Model Assembly Geometry* for model details). The first row of the table describes the different parameters and assembly types (clear wall and others are for full walls). The first column describes the stand-off shelf connector type, which is sorted as either a proprietary C-shaped bracket (Figure 3. Proprietary shelf angle support bracket or a knife plate system (Figure 4. Generic welded knife plate for shelf angle support). The second column describes the various exterior insulation thicknesses that were used in each assembly; the insulation thickness increases by 50.8 mm increments, from 101.6 mm to 254 mm. The third column describes HDG stand-off shelf connector (which is either the proprietary bracket or knife plate system), spaced at 1220 mm. The fourth column describes HDG stand-off shelf connector, spaced at 610 mm. The fifth column is for GFRP connectors, spaced at 1220 mm; this is specific to knife plate systems only, as a GFRP material has not been used for the proprietary brackets, therefore not applicable. The sixth column displays the heat flux density results for the clear wall assemblies.

Table 7. CMU backup simulation results, heat flux density q (W/m^2)

Stand-off Shelf Connector	**Exterior Insulation Thickness (mm)**	***Heat flux density q (W/m^2)***			
		HDG Connector, 1220 mm spacing	**HDG Connector, 610 mm spacing**	**GFRP Connector, 1220 mm spacing**	**Clear Wall**
Proprietary Bracket	101.6	11.39	13.03	N/A[1]	7.78
	152.4	8.37	10.14		5.28
	203.2	6.75	8.37		4.39
	254	5.63	7.22		3.66
Knife Plate	101.6	11.92	12.86	10.59	7.78
	152.4	8.43	9.45	7.36	5.28
	203.2	6.74	7.71	5.72	4.39
	254	5.65	6.58	4.68	3.66

[1]N/A: not applicable.

Table 8 displays the calculated linear transmittance results (see Section 3.2 for equations and example calculation) corresponding to whole wall configurations listed in Table 7.

Table 8. CMU backup simulation results, linear transmittance ψ (W/mK)

Stand-off Shelf Connector	***Linear transmittance ψ (W/mK)***			
	Exterior Insulation Thickness (mm)	**HDG Connector, 1220 mm spacing**	**HDG Connector, 610 mm spacing**	**GFRP Connector, 1220 mm spacing**
Proprietary Bracket	101.6	0.24	0.35	N/A[1]
	152.4	0.21	0.33	
	203.2	0.16	0.27	
	254	0.13	0.24	
Knife Plate	101.6	0.28	0.34	0.19
	152.4	0.21	0.28	0.14
	203.2	0.16	0.22	0.09
	254	0.13	0.20	0.07

[1]N/A: not applicable.

Using Equation 5 from *Section 3.2*, multipliers for thermal estimation are calculated using the heat flux density results in Table 7. Since heat flux density is inversely proportional to RSI or R-Values, the multipliers presented in the tables below may be applied to such if they are

inversed. Each listed scenario in the following tables for heat flux density and linear transmittance multipliers is defined by the changing parameter of the scenario and may be combined with each other for scenarios with more than one changing parameter.

Similar to Table 7 and Table 8, the first column of Table 9 describes the stand-off shelf connector type and the second column describes the exterior insulation thickness. Multipliers are then presented for Scenarios A_{CMU}, B_{CMU}, C_{CMU}, and D_{CMU} (the subscript defines the backup system). For scenarios A_{CMU} and B_{CMU} in Table 9 and Table 10 where insulation thickness is the changing parameter, it should be noted that the multiplier should be applied to the insulation thickness in the same row of the table, to resolve the heat flux density or linear transmittance of the insulation thickness of the next size/ row. This also explains the N/A in the 254 mm thickness row for Scenario A_{CMU} and B_{CMU} as the maximum insulation thickness studied was 254 mm. For example, under Scenario A_{CMU} of Table 9, if a user had the heat flux density of an assembly with 152.4 mm of insulation but the project required 203.2 mm of insulation, a multiplier with a value of 0.81 would be applied to the given model. This means the heat flux density of the assembly decreased by 19% when 50.8 mm of insulation was added (when using HDG proprietary brackets at 1220 mm spacing). Similarly, if the project required 254 mm of insulation, both a 0.81 and 0.83 multiplier would be applied to the given heat flux density. Scenario C_{CMU} presents multipliers for when HDG knife plates are changed to GFRP knife plates. Scenario D_{CMU} is for when the spacing of the stand-off shelf connectors decrease from 1200 mm to 610 mm. Again, the multipliers in Table 9 may be applied to heat flux density values, or thermal transmittance per unit area, u (W/m^2K) and of a given area U, (W/K) because they are directly proportional to each other. This can be further extended to other similar terms such as R-Value and RSI, in which the thermal transmittance of the assembly would be divided

by the multiplier (instead of being multiplied) since R-value is the inverse of thermal transmittance.

Table 9. CMU backup: heat flux density multipliers for thermal estimation

Stand-off Shelf Connector	**Insulation Thickness (mm)**	***Heat flux density multipliers***			
		Scenario A_{CMU}	**Scenario B_{CMU}**	**Scenario C_{CMU}**	**Scenario D_{CMU}**
		Insulation thickness[1,2]	**Insulation thickness[1,3]**	**HDG to GFRP connectors**	**1220 to 610 mm connector spacing**
Proprietary Bracket	101.6	0.73	N/A[4]	N/A[4]	1.14
	152.4	0.81			1.21
	203.2	0.83			1.24
	254	N/A[4]			1.28
Knife Plate	101.6	0.71	0.69	0.89	1.08
	152.4	0.80	0.78	0.87	1.12
	203.2	0.84	0.82	0.85	1.14
	254	N/A[4]	N/A[4]	0.83	1.17

[1]At 1220 mm spacing.
[2]HDG stand-off shelf angle connectors used.
[3]GFRP stand-off shelf angle connectors used.
[4]N/A: not applicable.

A separate table with multipliers to apply directly to linear transmittance values is shown in Table 10 because a linear transmittance reflects the difference between the heat flux of the full wall and clear wall (i.e. not directly proportional to a single heat flux density value). Linear transmittance multipliers for thermal estimation may be created by using the linear transmittance results from Table 8.

Table 10. CMU backup: linear transmittance multipliers for thermal estimation

Stand-off Shelf Connector	**Insulation Thickness (mm)**	***Linear transmittance multipliers***			
		Scenario A_{CMU}	**Scenario B_{CMU}**	**Scenario C_{CMU}**	**Scenario D_{CMU}**
		Insulation thickness[1,2]	**Insulation thickness[1,3]**	**HDG to GFRP connectors**	**1220 to 610 mm connector spacing**
Proprietary Bracket	101.6	0.88	N/A[4]	N/A[4]	1.46
	152.4	0.76			1.57
	203.2	0.81			1.69
	254	N/A[4]			1.85
Knife Plate	101.6	0.75	0.74	0.55	1.21
	152.4	0.76	0.64	0.50	1.33
	203.2	0.81	0.78	0.40	1.38
	254	N/A[4]	N/A[4]	0.35	1.54

[1]At 1220 mm spacing.
[2]HDG stand-off shelf angle connectors used.
[3]GFRP stand-off shelf angle connectors used.
[4]N/A: not applicable.

Example multiplier calculations:

(1) A ψ value of 0.26 W/mK is available for a CMU backup assembly with 101.6 mm (4") of mineral wool insulation. The project under investigation requires **203.2 mm (8")** of mineral wool insulation to meet code. **Proprietary brackets** with a HDG finish have been selected.

$$\psi_{final} = \psi_{given} \times M_{Scenario\ A}^{101.6\ mm} \times M_{Scenario\ A}^{152.4\ mm}$$

$$\psi_{final} = 0.26 \frac{W}{mK} \times 0.88 \times 0.76 = 0.17$$

(2) The **knife plate** spacing of a CMU backup assembly must be reduced from **1220 mm on center to 610 mm** to be able to support the vertical loads imposed on the system. The ψ value for a system with 101.6 mm of mineral wool insulation and 1220 mm on center spacing for **HDG** knife plates has been found to be 0.36 W/mK. The project also **requires 152.4 mm** of mineral wool insulation.

$$\psi_{final} = \psi_{given} \times M_{Scenario\ A}^{101.6\ mm} \times M_{Scenario\ D}^{152.4\ mm}$$

$$\psi_{final} = 0.36 \frac{W}{mK} \times 0.75 \times 1.33 = 0.36$$

It is interesting to note in this example that by increasing the insulation thickness, the linear transmittance of the knife plates are reduced by approximately 25%, but when the knife plate spacing is reduced from 1220 mm to 610 mm, the increase in linear transmittance is proportional to the reduction of the thicker insulation.

CMU backup discussion:

Exterior insulation thickness:

The simulation results for increasing exterior insulation thickness were as expected: the thicker the insulation, the lower the heat flux density through the wall assembly. This pattern is evident in all of the simulation results, including the clear wall assemblies. Note that the clear wall values are the same for the proprietary bracket and knife plate system because those connectors are removed in the clear wall assemblies.

Multipliers:

When calculating linear transmittance (ψ) values, it can be seen from the tables above that small differences in heat flux density can cause greater differences in ψ multiplier values. For example, when comparing multipliers for CMU backup in Table 9 and Table 10, the difference between the multipliers in Scenario C_{CMU} are much more apparent in Table 10 as compared to Table 9. Using Scenario C_{CMU}, focusing on the Knife Plate stand-off shelf connector with 152.4 mm of insulation, the multiplier for heat flux density is 0.87 while the multiplier for ψ is 0.50. This appears to be a very large difference upon first glance but it is how the ψ value is formulated that later makes up for this difference. The ψ value is dependent on the difference between the full wall and clear wall thermal transmittance values, which accounts for the small ψ value. The resultant ψ value is a much smaller value than heat flux density so small numerical differences will have a more pronounced effect on the overall value, which is why the ψ multiplier appears to be more dramatic than the q multiplier.

Stand-off shelf connector geometry:

The two stand-off shelf connectors that were modeled differ in configuration (cross-sectional geometry) but effectively function in the same way. The heat flux density values for the two stand-off shelf connector systems in Table 7 are very close in number; at a 1220 mm spacing, the difference between the two systems is almost negligible, ranging between 0.12 to 4.48%. This is reinforced in Table 8, where the ψ value for both stand-off shelf connector systems are identical with shown significant digits when the insulation thickness is greater than 101.6 mm. At a 610 mm spacing, the difference between the two systems becomes more prominent as insulation thickness increases, and the heat flux density difference ranges from 1.3 to 8.76%. The knife plate systems have lower thermal bridging effect, likely due to the dual

"fins" that protrude from the proprietary bracket, as the knife plate system only has one "fin". Although proprietary products often have a higher initial cost than conventional systems, it is worth mentioning that using knife plate systems require an engineer for design procurement and hiring additional welders on-site for installation. On-site welding has additional risks including pitting of glazing and other surfaces, and fires.

Stand-off shelf connector spacing:

Reducing the spacing between stand-off shelf angle connectors appears to have the greatest range of influence on thermal performance. Reducing the stand-off spacing from 1220 mm to 610 mm increases the heat flux density by 12.61% to 22.02% and 7.30% to 14.19% (when looking at 101.6 mm to 254 mm to insulation) for the proprietary brackets and knife plate system, respectively. Decreasing the spacing appears to have a greater effect as insulation thickness increases, and is slightly more pronounced in the proprietary brackets than knife plate system. This is referencing the sensitivity of the systems to decreasing their spacing because again, when looking at the actual difference between the two geometries (see previous paragraph), the final difference between the two systems are negligible (less than 10%).

HDG to GFRP material finish:

GFRP material has a significantly lower conductivity than HDG steel (0.2 W/mK for GFRP and 50 W/mK for HDG steel), so changing from HDG to GFRP knife plates will obviously reduce the thermal bridging through the assembly. The difference appears to be more significant as the insulation thickness increases, with improvements in heat flux density ranging from 11.16% with a 102 mm insulation thickness to 17.17% with a 254 mm insulation thickness. Again, it should be noted that the knife plate geometry in this study was not structurally designed for the intended loads shown in the models. It is a generic detail that may not be structurally

sufficient (especially for the thicker insulation sizes) and was constructed for the sake of thermal comparison of materials only. It is more realistic that a much larger contact area is required between the back up and shelf angle when using GFRP materials. There are current technologies that require a solid block of GFRP (or similar polymer) and a through-bolt to install.

4.2 ***Wood Stud Backup***

Table 11 displays the heat flux density results for the wood stud backup simulations. Only the proprietary bracket system was modeled for stand-off shelf connectors. In the second column, following construction practices, two different types of exterior insulation were modeled: XPS and mineral wool. The two different exterior insulation thicknesses are described in the third column. The fourth column describes the intermediate floor type, which is either wood (see Figure 9) or a concrete slab with a range of various conductivities. The conductivities modeled were 10 times (18 W/mK) and a tenth (0.18 W/mK) of the original intermediate concrete slab (1.8 W/mK), in order to present a range of results to determine the influence of slab conductivity over the total heat flux of the assembly. The fifth column describes the HDG proprietary bracket connector spaced at 1220 mm. The sixth column describes the HDG proprietary bracket connector spaced at 610 mm; only one insulation scenario was modeled for this parameter in order to compare to the 1200 mm spacing parameter. The seventh column presents the heat flux density results of the clear wall assemblies.

Table 11. Wood stud backup simulation results, heat flux density q (W/m²)

Stand-off Shelf Connector	**Exterior Insulation Type[1]**	**Exterior Insulation Thickness (mm)**	**Intermediate Floor Type (W/mK)**	***Heat flux density q (W/m²)***		
				HDG Connector, 1220 mm spacing	**HDG Connector, 610 mm spacing**	**Clear Wall**
Proprietary Bracket	XPS	50.8	Wood (see Figure 9)	7.50	7.51	7.19
		101.6		5.90	N/A[4]	5.65
	Mineral wool	50.8		7.87		7.54
		101.6		6.30		6.04[3]
	Mineral wool	101.6	Concrete (1.8)[2]	7.63		
			Concrete (0.18)	6.64		
			Concrete (18)	7.96		

[1]For interior insulation: space between wood studs has been filled with fiberglass batt insulation, see Section 3.1.1 for details.
[2]Actual thermal conductivity of concrete.
[3]Floor is not included in clear wall, see Section 3.1.1 for details.
[4]N/A: not applicable.

Table 12. Wood stud backup simulation results, linear transmittance ψ (W/mK)

Stand-off Shelf Connector	**Exterior Insulation Type[1]**	**Exterior Insulation Thickness (mm)**	**Flooring Type (W/mK)**	***Linear transmittance ψ (W/mK)***	
				HDG Connector, 1220 mm spacing	**HDG Connector, 610 mm spacing**
Proprietary Bracket	XPS	50.8	Wood (see Figure 9)	0.02	0.02
		101.6		0.02	N/A[3]
	Mineral wool	50.8		0.02	
		101.6		0.02	
	Mineral wool	101.6	Concrete (1.8)[2]	0.11	
			Concrete (0.18)	0.04	
			Concrete (18)	0.13	

[1]For interior insulation: space between wood studs has been filled with fiberglass batt insulation, see Section 3.1.1 for details.
[2]Actual thermal conductivity of concrete.
[3] N/A: not applicable.

To account for the relations between the three different conductivities of the intermediate concrete slab, multipliers were created between the low, medium/ normal, and high conductivities in Table 13. For example, if the project has a low intermediate slab conductivity (0.18 W/mK) and the designer wanted to see the heat flux density difference if a high

intermediate slab conductivity (18 W/mK) was implemented, a multiplier of 1.20 could be applied. This means the heat flux density would increase by 20% if the intermediate slab was changed from a low to high conductivity. To obtain a multiplier in the opposite direction (i.e. from high conductivity to low conductivity), take the inverse of the multiplier (1/1.20 = 0.83).

Table 13. Wood stud backup: heat flux density multipliers based on intermediate slab conductivity

Conductivity (W/mK)	Heat flux density multipliers
Low (0.18) to Medium/ Normal (1.8)	1.15
Low (0.18) to High (18)	1.20
Medium/ Normal (1.8) to High (18)	1.04

The multipliers for thermal estimation for a wood stud backup are separated by scenario as before. Scenario A_{wood} presents multipliers for changing from 50.8 mm to 101.6 mm of exterior insulation. Scenario B_{wood} presents multipliers from changing from XPS to mineral wool insulation. Scenario C_{wood} presents a multiplier for changing proprietary bracket spacing from 1220 mm to 610 mm spacing, with 50.8 mm of exterior XPS insulation. And finally, Scenario D_{wood} presents a multiplier for changing the intermediate flooring from wood (see Figure 9) to a concrete slab, with 101.6 mm of exterior mineral wool insulation.

Table 14. Wood stud backup: heat flux density multipliers for thermal estimation

<table>
<tr><th rowspan="3">Insulation Type</th><th rowspan="3">Exterior Insulation Thickness (mm)</th><th colspan="4">Heat flux density multipliers</th></tr>
<tr><th>Scenario A_{wood}[1]</th><th>Scenario B_{wood}[1]</th><th>Scenario C_{wood}[1]</th><th>Scenario D_{wood}[1]</th></tr>
<tr><th>50.8 to 101.6 mm of exterior insulation[2]</th><th>XPS to mineral wool insulation[2]</th><th>1220 to 610 mm spacing</th><th>Wood floor to concrete slab[2]</th></tr>
<tr><td rowspan="2">XPS</td><td>50.8</td><td rowspan="2">0.79</td><td>1.05</td><td>1.00</td><td rowspan="2">N/A[3]</td></tr>
<tr><td>101.6</td><td>1.07</td><td rowspan="2">N/A[3]</td></tr>
<tr><td rowspan="2">Mineral Wool</td><td>50.8</td><td rowspan="2">0.80</td><td rowspan="2">N/A[3]</td></tr>
<tr><td>101.6</td><td>1.21</td></tr>
</table>

[1]HDG proprietary bracket stand-off shelf angle connectors used in all scenarios.
[2]At 1220 mm spacing.
[3] N/A: not applicable.

Table 15. Wood stud backup: linear transmittance multipliers for thermal estimation

Insulation Type	**Exterior Insulation Thickness (mm)**	***Linear transmittance multipliers***			
		Scenario A_{wood}[1]	**Scenario B_{wood}[1]**	**Scenario C_{wood}[1]**	**Scenario D_{wood}[1]**
		50.8 to 101.6 mm of exterior insulation[2,3]	**XPS to mineral wool insulation[2,3]**	**1220 to 610 mm spacing[3]**	**Wood floor to concrete slab[2]**
XPS	50.8	0.78	1.05	1.01	N/A[4]
	101.6		1.04	N/A[4]	
Mineral Wool	50.8	0.81	N/A[4]		
	101.6				6.21

[1]HDG proprietary bracket stand-off shelf angle connectors used in all scenarios.
[2]At 1220 mm spacing.
[3]With wood flooring.
[4]N/A: not applicable.

Wood stud backup discussion:

Exterior insulation type and thickness:

Two different exterior insulation types were modeled in the wood stud backup assemblies. XPS is more commonly used in-practice with wood stud backup systems, but mineral wool was still modeled in order to compare results across different assembly types in Section 4.4 *Cross-backup Relationships*, as mineral wool is common in-practice for other backup types like CMU and steel stud. XPS has a slightly lower conductivity than mineral wool (0.029 W/mK for XPS and 0.034 W/mK for mineral wool), therefore presenting higher values of thermal resistance than mineral wool, at the same thickness size. In both the full wall and clear wall assemblies, mineral wool insulation is 5% less effective in terms of reducing the heat flow through the assembly than XPS at 50.8 mm thickness and 7% less effective than XPS at 101.6 mm thickness. The linear transmittance results of the proprietary bracket, with a wood intermediate floor are all the same value regardless of insulation type and thickness. This is not surprising as the wood stud flooring has a low conductivity and the heat transferred from the interior to exterior that reaches the proprietary brackets is already a small amount. When

comparing the heat flux density values in Table 11, column **HDG Connector, 1220 mm** spacing and **Clear Wall**, the values are close, inferring that the proprietary bracket and wood intermediate floor is not a significant thermal bridge. This is further reinforced in the paragraph below as well.

Stand-off shelf connector spacing:

The heat flux density when changing the proprietary bracket spacing from 1220 mm to 610 mm makes an insignificant difference, mainly due to the low conductivity of the wood intermediate flooring.

Intermediate floor type:

Decreasing the conductivity of the intermediate concrete slab by a factor of 10, decreases the heat flux density by 13%. Increasing the conductivity of the intermediate concrete slab by a factor of 10, increases the heat flux density by 4.2%. Alternatively said, decreasing the conductivity of the intermediate concrete slab by a factor of 10, decreases the linear transmittance by 62%. Increasing the conductivity of the intermediate concrete slab by a factor of 10, increases the linear transmittance by 18%. This infers that the assembly is more sensitive to changes that decrease the intermediate floor conductivity. The results show that if the intermediate floor has very low thermal conductivity (i.e. wood) then the thermal bridging is minimized and changes to insulation thickness or connector spacing creates negligible differences. The reason why the heat flux density or linear transmittance does not change significantly when increasing the conductivity of the intermediate concrete slab by a factor of 10 is likely because the concrete itself does not have a low conductivity as compared to insulation – thus allowing most heat to already flow through it, so when the conductivity further increases,

the change is little. On the other hand, when the intermediate concrete slab conductivity is decreased by a factor of 10, the change is dramatic because the heat flow from the interior to the connectors is significantly reduced. In this case, the spacing of the connectors will be significant.

Additional wood stud at grade assemblies are provided in **Appendix A**, *Section A.3, Additional wood stud at-grade* models. The models presented in **Section 4, Results and Discussion** all contain intermediate slabs, which are different than at-grade models that have foundation walls. Foundation walls have a greater projection into the ground, and as shown in **Appendix A**, the geometry of the at-grade slab is 703 mm from the top of slab to the bottom of foundation wall (i.e. 203 mm concrete slab thickness with a 500 mm projection into the ground). It was found that the heat flux and linear transmittance value is higher in the at-grade models, as compared with the intermediate floor at the same insulation thickness. This is not surprising as the concrete slab wall (also 203 mm thick) has replaced the components with a higher thermal resistivity (e.g. wood studs and fiberglass batt insulation in-between the studs).

4.3 ***Steel Stud Backup***

The heat flux results for the steel stud backup simulations are presented below in Table 16. The first column describes the stand-off shelf connectors, where both the proprietary bracket and knife plates were modelled. The second column indicates the exterior insulation thicknesses, from 101.6 mm to 203.2 mm, in 50.8 mm increments. The third column presents simulations results for HDG connectors at a 1220 mm spacing. The fourth column presents results for GFRP knife plates at 1220 mm spacing (again, the proprietary brackets were not modeled with a GFRP finish as they are not available in that material finish). The fifth column presents clear wall results for the metal stud backup.

Table 16. Steel stud backup simulation results, heat flux density q (W/m^2)

Stand-off Shelf Connector	**Exterior Insulation Thickness (mm)**	***Heat flux density q (W/m^2)***		
		HDG Connector, 1220 mm spacing	**GFRP Connector, 1220 mm spacing**	**Clear Wall**
Proprietary Bracket	101.6	12.11	N/A[1]	11.27
	152.4	9.54		9.01
	203.2	7.58		7.50
Knife Plate	101.6	12.49	11.31	11.27
	152.4	9.52	N/A[1]	9.01
	203.2	7.88		7.50

[1]N/A: not applicable

Table 17. Steel stud backup simulation results, linear transmittance ψ (W/mK)

Stand-off Shelf Connector	**Exterior Insulation Thickness (mm)**	***Linear transmittance ψ (W/mK)***	
		HDG Connector, 1220 mm spacing	**GFRP Connector, 1220 mm spacing**
Proprietary Bracket	101.6	0.057	N/A[1]
	152.4	0.036	
	203.2	0.0052	
Knife Plate	101.6	0.083	0.0029
	152.4	0.034	N/A[1]
	203.2	0.026	

[1]N/A: not applicable

Scenario A_{steel} Table 18 and Table 19 presents multipliers for when insulation thickness is the changing parameter. Again, it should be noted that the multiplier is applied to the insulation thickness in the current row, to resolve the heat flux density or linear transmittance of the insulation thickness of the next size/ row. This explains the N/A in the 203.2 mm thickness row for Scenario A_{steel} as the maximum insulation thickness in the steel stud backup simulations were 203.2 mm. Scenario B_{steel} multipliers are applied when knife plate systems are being switched from HDG to GFRP.

Table 18. Steel stud backup: heat flux density multipliers for thermal estimation

Stand-off Shelf Connector	**Insulation Thickness (mm)**	***Heat flux density multipliers***	
		Scenario A_{steel}	**Scenario B_{steel}**
		Insulation thickness[1,2]	**HDG to GFRP connectors**
Proprietary Bracket	101.6	0.79	N/A[3]
	152.4	0.79	
	203.2	N/A[3]	
Knife Plate	101.6	0.76	0.91
	152.4	0.83	N/A[3]
	203.2	N/A[3]	

[1]At 1220 mm spacing.
[2]HDG stand-off shelf angle connectors used.
[3]N/A: not applicable.

Table 19. Steel stud backup: linear transmittance multipliers for thermal estimation

Stand-off Shelf Connector	**Insulation Thickness (mm)**	***Linear transmittance multipliers***	
		Scenario A_{steel}	**Scenario B_{steel}**
		Insulation thickness[1,2]	**HDG to GFRP connectors**
Proprietary Bracket	101.6	0.63	N/A[3]
	152.4	0.14	
	203.2	N/A[3]	
Knife Plate	101.6	0.42	0.04
	152.4	0.74	N/A[3]
	203.2	N/A[3]	

[1]At 1220 mm spacing.
[2]HDG stand-off shelf angle connectors used.
[3]N/A: not applicable.

Steel stud backup discussion:

Exterior insulation thickness:

Similar to the CMU backup, as the insulation thickness increases, the heat flux density decreases. This pattern is evident in all of the simulation results, including the clear wall assemblies. Note that the clear wall values are the same for the proprietary bracket and knife plate system because those connectors are removed in the clear wall assemblies.

Stand-off shelf connector geometry:

Similar to the CMU backup, there are negligible differences between the two stand-off shelf connector systems, with heat flux density differences ranging between 0.18 to 3.85%.

HDG to GFRP material finish:

Interestingly, it was found that the simulations with GFRP knife plates had heat flux density values extremely close to its clear wall value. Because of this, the linear transmittance is nearly zero. The remaining assemblies with thicker insulation were not modeled with GFRP knife plates because the thermal bridging effect of using this system is effectively negligible. This result is largely attributed to the backup system type. As opposed to the low conductivity of the wood stud backup in the previous section, a steel stud backup is highly conductive due to its material properties. Additionally, masonry ties are attached directly to the steel studs, which becomes a more significant point of thermal bridging as compared to the other backup systems because steel studs are significantly more conductive than CMU and wood. The steel stud back up starts off with a higher heat flux density value prior to any thermal bridging effects, due to the highly conductive steel studs, so although the linear transmittance value of the GFRP may seem low in comparison to others, it's because the heat has already been lost at other places within the assembly. The GFRP knife plate is not acting like a thermal bridge due to its inherent low conductivity and highly conductive environment. The general takeaway from this model is that GFRP knife plates on a steel stud back up system are not considered a thermal bridge as its linear transmittance is nearly zero.

4.4 ***Cross-backup Relationships***

Additional multipliers for changing between the CMU, wood stud, and steel stud backup types (see *Section 3.1.1 Physical and Model Assembly Geometry* for details), using exterior mineral wool insulation ranging from 101.6 mm to 203.2 mm, and in increments of 50.8 mm. They are presented below in Table 20. Note that only concrete intermediate floors were modeled for the CMU and steel stud backups. For wood stud backups, both a concrete and wood intermediate floor were modeled and is indicated with a superscript.

Table 20. Heat flux density multipliers for various backups with exterior mineral wool insulation

<table>
<tr><th rowspan="2">Stand-off Shelf Connector</th><th rowspan="2">Exterior Mineral Wool Insulation Thickness (mm)</th><th colspan="5">Heat flux density multipliers</th></tr>
<tr><th>CMU to Wood_{fl_wood}[1]</th><th>CMU to Wood_{fl_cnc}[2]</th><th>CMU to Steel</th><th>Wood_{fl_wood}[1] to Steel</th><th>Wood_{fl_cnc}[2] to Steel</th></tr>
<tr><td rowspan="3">Proprietary Bracket (HDG)</td><td>101.6</td><td>0.55</td><td>0.67</td><td>1.06</td><td>1.92</td><td>1.59</td></tr>
<tr><td>152.4</td><td colspan="2" rowspan="2">N/A[3]</td><td>1.14</td><td colspan="2" rowspan="2">N/A[3]</td></tr>
<tr><td>203.2</td><td>1.12</td></tr>
<tr><td rowspan="3">Knife Plate (HDG)</td><td>101.6</td><td>0.53</td><td>0.64</td><td>1.07</td><td>2.02</td><td>1.67</td></tr>
<tr><td>152.4</td><td colspan="2" rowspan="4">N/A[3]</td><td>1.13</td><td colspan="2" rowspan="4">N/A[3]</td></tr>
<tr><td>203.2</td><td>1.17</td></tr>
<tr><td rowspan="3">Knife Plate (GFRP)</td><td>101.6</td><td>1.07</td></tr>
<tr><td>152.4</td><td rowspan="2">N/A</td></tr>
<tr><td>203.2</td></tr>
</table>

[1] Wood$_{fl_wood}$ means wood stud backup with a wood intermediate floor.

[2]Wood$_{fl_cnc}$ means wood stud backup with a concrete intermediate floor.

[3]N/A: not applicable; the only exterior mineral wool insulation thickness modeled for wood stud was 4" as it is not realistic to go any thicker in mineral wool insulation with a wood stud backup

The intermediate floor type is not accounted for in the clear wall assemblies in Table 21 because intermediate floors are not modeled in clear wall assemblies.

Table 21. Heat flux density multipliers for clear wall assemblies using mineral wool insulation

Exterior Mineral Wool Insulation Thickness (mm)	***Heat flux density multipliers***		
	CMU to Wood	**CMU to Steel**	**Wood to Steel**
101.6	0.78	1.45	1.56
152.4	N/A[1]	1.70	N/A[1]
203.2		1.71	

[1]N/A: not applicable; the only exterior mineral wool insulation thickness modeled for wood stud was 4" as it is not realistic to go any thicker in mineral wool insulation with a wood stud backup.

Table 22. Linear transmittance multipliers for backups with exterior mineral wool insulation

Stand-off Shelf Connector	**Exterior Mineral Wool Insulation Thickness (mm)**	***Linear transmittance multipliers***				
		CMU to $Wood_{fl\_wood}$[1]	**CMU to $Wood_{fl\_cnc}$[2]**	**CMU to Steel**	**$Wood_{fl\_wood}$[1] to Steel**	**$Wood_{fl\_cnc}$[2] to Steel**
Proprietary Bracket (HDG)	101.6	0.07	0.45	0.24	3.23	0.52
	152.4	N/A[3]		0.17	N/A[3]	
	203.2			0.03		
Knife Plate (HDG)	101.6	0.06	0.39	0.30	4.68	0.75
	152.4	N/A[3]		0.17	N/A[3]	
	203.2			0.03		
Knife Plate (GFRP)	101.6			0.02		
	152.4			N/A		
	203.2					

[1] $Wood_{fl\_wood}$ means wood stud backup with a wood intermediate floor.

[2]$Wood_{fl\_cnc}$ means wood stud backup with a concrete intermediate floor.

[3]N/A: not applicable; the only exterior mineral wool insulation thickness modeled for wood stud was 4" as it is not realistic to go any thicker in mineral wool insulation with a wood stud backup.

Cross-backup relationships discussion:

The multipliers in Table 20 to Table 22 shows how influential the backup type is on the heat flux and linear transmittance of the assembly. It is evident that the multiplier will be less than 1 when either CMU or steel stud is being changed to wood stud because the heat flux density will always be the least in wood stud assemblies (in comparison to the others) because of its low conductivity. Conversely, when CMU or wood stud is being changed to steel stud, the multiplier will be greater than 1 because the CMU and steel stud backup has a higher heat flux

density due to its higher conductivity. Taking the reciprocal of the multipliers allows the scenario to be switched from one direction to the other. For example, in Table 20 the column **CMU to Wood$_{fl_wood}$** with a proprietary bracket (HDG) has a heat flux multiplier 0.55. If the scenario needed to be switched from **Wood$_{fl_wood}$ to CMU**, taking the reciprocal of 0.55 would give us the necessary multiplier of 1.82. Comparing this to the **Wood$_{fl_wood}$ to Steel** scenario with a q multiplier of 1.92, we can see that a CMU backup allows about 82% more heat to pass through its assembly than and a wood stud backup with wood intermediate floor, and 92 % for a steel stud backup. For a wood stud backup with a concrete intermediate floor, a CMU backup allows 49% more heat to pass through its assembly and a steel stud backup allows 59%. The difference from CMU to steel is not as nearly significant, only 6%, at the same 101.6 mm of exterior insulation. With thicker insulation like 152.4 mm and 203.2 mm, the multipliers do not vary much either. There are negligible differences between the HDG and GFRP knife plate multipliers, both in direct comparison and in general. This suggests that the stand-off shelf connector type and insulation thickness are not significant parameters when changing from a CMU to steel stud backup, and an average q multiplier could be applied regardless of system type or insulation thickness.

If neglecting the intermediate floor, we can compare the heat flux density multipliers in Table 21 which evaluates only the clear wall assemblies. Wood to CMU is 1.28, Wood to Steel is 1.56, and CMU to Steel is 1.48. The trends seen here are similar to the ones seen in Table 20, such as the largest difference being between Wood to Steel, then CMU to Steel, and then Wood to CMU being the smallest difference between backup types. What should be noted are the value of the multipliers in Table 21 as compared to Table 20. In Table 20, the multipliers in the CMU to Steel column are on the lower end from 1.06 to 1.17 whereas the multipliers in Table 21

for CMU to Steel range from 1.45 to 1.71. This is because the clear wall values of the two backup types are significantly different; the steel stud backup starts off with a high clear wall heat flux density value and slightly increases with the addition of linear transmittances. The CMU backup starts off with a low(er) clear wall heat flux density value and significantly increases with the addition of linear transmittances. This indicates that a CMU backup is more sensitive to linear transmittances than a steel stud backup, as a steel stud wall already starts off with a high clear wall heat flux density thus it cannot lose as much heat to thermal bridging as compared to the CMU backup.

5 Conclusion

Energy modeling and thermal bridging calculations have quickly become standardized practices within building design due to its influence in building energy consumption. The thermal bridging phenomenon, which was previously overlooked as insignificant areas of energy loss, are now realized as large contributors due to the importance of proper building envelope design. Currently, thermal bridging calculations are often inaccessible due to cost, time, and required skill-set. Because of this, thermal bridging catalogues have been made publicly available for engineers/ architects/ designers by authors who have the skill-set to do so. A building envelope has many components and parameters that can affect the heat flow through the assembly, and creating a new model or simulation for a minor parameter change can be time consuming and costly. This paper presents 3D thermal computer simulations with a focus on varying parameters such as insulation thickness, stand-off shelf angle connector configuration (proprietary bracket and traditional knife plates), stand-off material (Hot-Dipped Galvanized (HDG) Steel and Glass Fibre Reinforced Polymer (GFRP)), stand-off spacing (1.22m and 0.610m), and structural backups (concrete masonry unit, wood stud, and steel stud) to establish a numerical relationship (i.e. numerical multiplier) that accounts for these various parameters to capture a range of scenarios, rather than presenting a single value or a single scenario. The outcomes of this research include accurate, precise heat flux and linear transmittance results of exterior walls with brick veneer simulations to be used independently or in conjunction with the BETB; a study on the influence of shelf angles and how certain parameters (insulation thickness, material type, geometries, and structural backup types) affects the heat flux through the masonry assemblies.; and an alternative method in determining the thermal bridging effects of shelf angles on various types of masonry wall assemblies, with the

intent of providing results in a timely manner and for general precision to be used during the design phase of a project.

Within the parametric assessment, a key finding between the two stand-off shelf connectors was that the difference between the two systems is almost negligible, in terms of heat flow through the assembly, and where the stand-off shelf connector type was the only parameter change. As for stand-off shelf connector spacing, the result of a decreased spacing is more pronounced with higher-conductive backup systems such as steel stud and CMU and is negligible for a wood stud back up system. For a wood stud backup, the linear transmittance results of the proprietary bracket, with a wood intermediate floor are close regardless of insulation type and thickness. This is not surprising as the wood stud flooring has a high conductivity and the heat transferred from the interior to exterior that reaches the proprietary brackets is already a small amount. Simulations that altered the intermediate floor type on a wood stud backup found that the assembly is more sensitive to changes that decrease the intermediate floor conductivity. The results show that if the intermediate floor has very low thermal conductivity (i.e. wood) then the thermal bridging is minimized and changes to insulation thickness or connector spacing creates negligible differences. Additionally, changing from HDG knife plates to GFRP material reduces the heat flow through a CMU backup (although it is still considered a thermal bridge). But in the case of a steel stud backup, the GFRP knife plate cannot be considered a thermal bridge as its linear transmittance value is nearly zero. This effect is largely attributed to the highly conductive metal stud backup type. The steel stud back up starts off with a higher heat flux density value prior to any thermal bridging effects, so although the linear transmittance value of the GFRP may seem low in comparison to others, it's because the heat has already been lost at other places within the assembly. When looking at

cross-backup relationships, there are negligible differences between the HDG and GFRP knife plate multipliers. This suggests that the stand-off shelf connector type and insulation thickness are not significant factors when changing from a CMU to steel stud backup, and an average multiplier could be applied regardless of system type or insulation thickness. It was also found that a CMU backup is more sensitive to linear transmittances than a steel stud backup, as a steel stud wall already starts off with a high clear wall heat flux density thus it cannot lose as much heat to thermal bridging as compared to the CMU backup.

5.1 ***Limitations***

The largest limitation of this research was that the simulations were not validated against real experiments as planned, due to lab closures regarding COVID-19. All simulations are user-controlled from every aspect of planning, including all input features so the results are heavily reliant on the user. Ideally, one could verify against experimental results to compare the simulation and then have the opportunity to adjust the model to account for unprecedented external influences. But in cases like this, validation occurs based on previous similar studies/ simulations. An additional limitation of this study is the number and type of parameters studied. Every single component of the wall assembly has the capacity to influence the overall thermal transmittance through the wall. The purpose of this study was to focus on a few key parameters that were suspected to have a large influence, but could be expanded to include either an extended list of sizes or completely new parameters. Another limitation includes the idealization of building component geometries and installations. The building materials used in the assemblies are highly variable in-field in terms of both geometry and installation procedure. Most often models will present or account for the worst-case-scenario but in practice, a completely new variation will always occur. Also, as mentioned earlier, the knife plates

modeled in this research were not structurally tested or modeled to account for the loads in the assembly. This is because there is a very large range of possible brick loads and backup loading capabilities that are unique to every project so the possibilities are endless. A generic knife-plate size was chosen, although not validated so this is an additional limitation. There is also a range of possibilities in CMU thermal conductivities due to differences in grout mixtures, and a simplified method (or table) to determine the equivalent conductivity for a fully or partially grouted CMU block based on the grout mixture can minimize discrepancies. Actual measured conductivities using an environmental chamber or similar measuring apparatus would be ideal. For the work in this thesis, a reasonable range for CMU conductivity is practical because an entire wall is being evaluated. In the case of a more refined evaluation (e.g. a single CMU block), the exact conductivity may be necessary.

5.2 ***Future Research***

This research can be expanded to include many other various parameters and more typical backup type configurations such as at-grade, parapet, or corner details. It would be beneficial to the research timeline to automate the modeling process using a script or code, and to integrate an artificial intelligence techniques to identify key parameters that affect the heat flow through the assembly once the database is large enough. To address the stand-off shelf connector detail, from both a thermal and structural perspective, it would be beneficial to structural engineers to create a design guide in which an optimal knife plate detail could be designed where parameters such as structural integrity, thermal conductivity, and cost could be optimized, based on project details such as design load and backup system. And more generally, due to the range of variability in simulations, it can also be suggested that additional verification can be done by other modelers using the same or different program/ methods.

6 References

1. Alhawari, A. and P. Mukhopadhyaya (2018). "Thermal bridges in building envelopes - An overview of impacts and solutions." International Review of Applied Sciences and Engineering **9**: 31-40.
2. American Society of Heating Refrigerating and Air-Conditioning Engineers (2009). 2009 ASHRAE Handbook: fundamentals. Atlanta, GA.
3. American Society of Heating Refrigerating and Air-Conditioning Engineers (2017). 2017 ASHRAE Handbook: fundamentals. Atlanta, GA.
4. Anderson, J., J. D'aloisio, D. DeLong, R. Miller-Johnson, K. Oberdorf, R. Ranieri, T. Stine and G. Weisenberger (2012). Thermal Bridging Solutions: Minimizing Structural Steel's Impact on Building Envelope Energy Transfer. Modern Steel Construction, American Institute of Steel Construction,**:** 16.
5. Asdrubali, F., G. Baldinelli and F. Bianchi (2011). A quantitative methodology to evaluate thermal bridges in buildings. Third International Conference on Applied Energy. Perugia, Italy.
6. ASHRAE (2019). ANSI/ASHRAE/ IES Standard 90.1-2019-- Energy Standard for Buildings Except Low-Rise Residential Buildings (I-P Edition).
7. Canadian Concrete Masonry Producers' Association Metric Technical Manual: Section 6. Thermal Properties and Design Details.
8. Desjarlais, A. O. and A. G. McGowan (1997). Comparison of Experimental and Analytical Methods to Evaluate Thermal Bridges in Wall Systems. 3rd ASTM Symposium. Quebec. **Third:** 15.

9. Dimitrov, A. V. (2015). Energy Modeling and Computations in the Building Envelope. Bova Raton, CRC Press.
10. Dodoo, A., L. Gustavsson and R. Sathre (2011). "Building energy-efficiency standards in a life cycle primary energy perspective." Energy & Buildings **43**: 1589-1597.
11. Fernandes, P. M. d. O. (2014). Thermal Characterization of Glass Fibre Reinforced Polmer (GFRP) Sandwich Panels. U. D. L. Instituto Superior Tecnico. Lisbon, Portugal.
12. Finch, G., M. Wilson and J. Higgins (2013). Thermal Bridging of Masonry Veneer Claddings and Energy Code Compliance. 12th Canadian Masonry Symposium. Vancouver BC**:** 12.
13. Hassid, S. (1990). "Thermal Bridges Across Multilayer Walls: An Integral Approach." Building and Environment **25**: 143-150.
14. Ibn-Mohammed, T., R. Greenough, S. Taylor, L. Ozawa-Meida and A. Acquaye (2013). "Operational vs. embodied emissions in buildings—A review of current trends." Energy & Buildings **66**: 232-245.
15. International, A. (2011). ASTM C1363-11, Standard Test Method for Thermal Performance of Building Materials and Envelope Assemblies by Means of a Hot Box Apparatus. West Conshohocket, PA.
16. International Organization for Standardization (2017). Thermal bridges in building construction - Linear thermal transmittance - Simplified methods and default values. ISO 14683. Switzerland.
17. International Panel on Climate Change (2014). "Climate Change 2014: Mitigation of Climate Change."

18. Kim, H. and M. Yeo (2020). "Thermal Bridge Modeling and a Dynamic Analysis Method Using the Analogy of a Steady-State Thermal Bridge Analysis and System Identification Process for Building Energy Simulation: Methodology and Validation." energies **13**.
19. Love, A. and C. Klee "Thermal Bridging: Observed Impacts and Proposed Improvement for Common Conditions."
20. Martin, K., A. Erkoreka, I. Flores, M. Odriozola and J. M. Sala (2010). "Problems in the calculation of thermal bridges in dynamic conditions." Elsevier **Energy and Buildings 43**: 529-535.
21. Mason Contractors Association of America. (2021). "Structural Backup." Retrieved April 27, 2021, from https://www.masoncontractors.org/glossary/structural-backup/.
22. Morrison Hershfield Limited (2019). Building Envelope Thermal Bridging Guide (V1.3).
23. Morrison Hershfield Limited (2020). Building Envelope Thermal Bridging Guide (V1.4).
24. Morrison Hershfield Limited (2020). Building Envelope Thermal Bridging Guide (V1.5).
25. National Research Council of Canada (2011). National Energy Code of Canada for Buildings 2011. Ottawa, Natural Resources Canada,.
26. National Research Council of Canada (2017). National Energy Code of Canada for Buildings 2017. Ottawa, Natural Resources Canada,.
27. Natural Resources Canada (2018a). Residential Sector, Canada, Table 2: Secondary Energy Use and GHG Emissions by End-Use.
28. Natural Resources Canada (2018b). Commercial/ Institutional Sector, Canada, Table 4: Secondary Energy Use and GHG Emissions by End-Use - Including Electricity-Related Emissions.
29. Patrick Roppel, W. M. (2011). ASHRAE Research Project Report, RP-1365.

30. Placido, A. D., B. Brown, D. Chong and C. Schumacher (2019). Thermal Evaluation of Masonry Shelf Angle Supports for Exterior-Insulated Walls. 2019 Building XIV International Conference. Clearwater Beach, Florida**:** 9.
31. Quinten, J. and V. Feldheim (2015). "Dynamic modelling of multidimensional thermal bridges in building envelopes: Review of existing methods, application and new mixed method." Elsevier **110**: 284-293.
32. Ruparathna, R., K. Hewage and R. Sadiq (2016). "Improving the energy efficiency of the existing building stock: A critical review of commercial and institutional buildings." Elsevier **53**: 1032-1045.
33. The Government of Newfoundland and Labrador (2016). Guide to better building envelopes for large buildings.
34. United States Department of Energy (2012). Buildings Energy Data Book. U. S. D. o. Energy.

7 Appendix A

A.1 Additional Figures

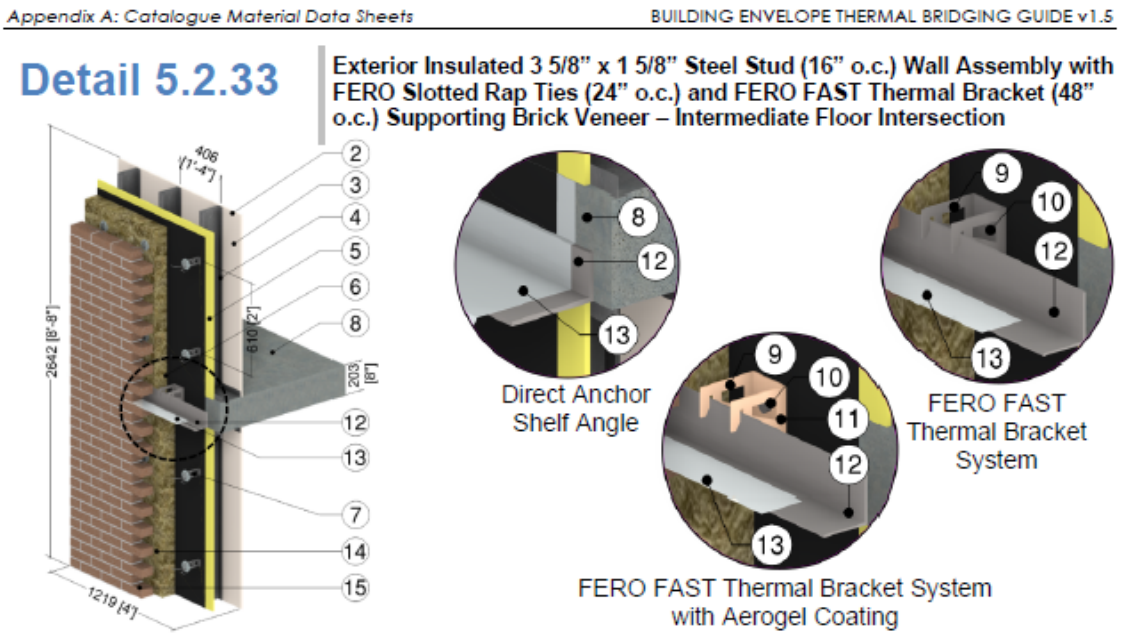

ID	Component	Thickness Inches (mm)	Conductivity Btu·in / ft²·hr·°F (W/m K)	Nominal Resistance hr·ft²·°F/Btu (m²K/W)	Density lb/ft³ (kg/m³)	Specific Heat Btu/lb·°F (J/kg K)
1	Interior Film[1]	-	-	R-0.7 (0.12 RSI)	-	-
2	Gypsum Board	1/2" (13)	1.1 (0.16)	R-0.5 (0.08 RSI)	50 (800)	0.26 (1090)
3	Air in Stud Cavity	3 5/8" (92)	-	R-0.9 (0.16 RSI)	0.075 (1.2)	0.24 (1000)
4	3 5/8" x 1 5/8" Steel Studs with Top and Bottom Tracks	20 Gauge	430 (62)	-	489 (7830)	0.12 (500)
5	Exterior Sheathing	1/2" (13)	1.1 (0.16)	R-0.5 (0.08 RSI)	50 (800)	0.26 (1090)
6	Exterior Insulation	4" (102)	varies	R-16.8 (2.96 RSI) to R-24.0 (4.23 RSI)	varies	varies
7	Brick Ties	4" (102)	430 (62)	-	445 (7130)	0.09 (390)
8	Intermediate Concrete Floor	8" (203)	12.5 (1.8)	-	140 (2250)	0.20 (850)
9	FERO FAST Bracket	3/16" (5)	347 (50)	-	489 (7830)	0.12 (500)
10	Anchor Bolt	5/8" (16) Ø	347 (50)	-	489 (7830)	0.12 (500)
11	Aerogel Coating	1/8" (3)	0.24 (0.035)	-	-	-
12	Shelf Angle	3/8" (10)	347 (50)	-	489 (7830)	0.12 (500)
13	Flashing	20 Gauge	430 (62)	-	489 (7830)	0.12 (500)
14	Vented Air Cavity	1" (25)	-	R-0.4 (0.07 RSI)	0.075 (1.2)	0.24 (1000)
15	Brick Veneer	3 5/8" (92)	5.4 (0.78)	-	120 (1920)	0.19 (720)
16	Exterior Film[1]	-	-	R-0.2 (0.03 RSI)	-	-

[1] Value selected from table 1, p. 26.1 of 2009 ASHRAE Handbook – Fundamentals depending on surface orientation

Figure 12. Detail 5.1.89 from Appendix A of the Building Envelope Thermal Bridging Guide (Morrison Hershfield Limited 2020)

Detail 5.2.33

Exterior Insulated 3 5/8" x 1 5/8" Steel Stud (16" o.c.) Wall Assembly with FERO Slotted Rap Ties (24" o.c.) and FERO FAST Thermal Bracket (48" o.c.) Supporting Brick Veneer – Intermediate Floor Intersection

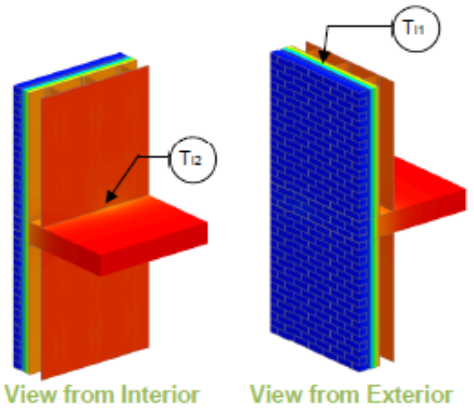

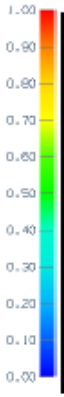

Thermal Performance Indicators

Assembly 1D (Nominal) R-Value	R_{1D}	R-4.3 (0.76 RSI) + exterior insulation
Transmittance / Resistance without Anomaly	U_o, R_o	"clear wall" U- and R-value without slab and shelf angle
Transmittance / Resistance	U, R	U- and R-values for overall assembly
Surface Temperature Index[1]	T_I	0 = exterior temperature 1 = interior temperature
Linear Transmittance	ψ	Incremental increase in transmittance per linear length of slab with shelf angle

Scenario

Scenario	Shelf Angle
1	Direct Anchor Shelf Angle
2	FERO FAST Thermal Bracket System
3	FERO FAST Thermal Bracket with Aerogel Coating

Nominal (1D) vs. Assembly Performance Indicators

Scenario	Exterior Insulation 1D R-Value (RSI)	R_{1D} ft²·hr·°F / Btu (m² K / W)	R_o ft²·hr·°F / Btu (m² K / W)	U_o Btu/ft²·hr·°F (W/m² K)	R ft²·hr·°F / Btu (m² K / W)	U Btu/ft²·hr·°F (W/m² K)	ψ Btu/ft hr °F (W/m K)
1	R-16.8 (2.96)	R-21.1 (3.72)	R-18.6 (3.28)	0.054 (0.305)	R-10.8 (1.90)	0.093 (0.525)	0.337 (0.583)
	R-24.0 (4.23)	R-28.3 (4.98)	R-24.1 (4.25)	0.041 (0.235)	R-12.2 (2.15)	0.082 (0.466)	0.351 (0.608)
2	R-16.8 (2.96)	R-21.1 (3.72)	R-18.6 (3.28)	0.054 (0.305)	R-16.7 (2.94)	0.060 (0.341)	0.055 (0.095)
	R-24.0 (4.23)	R-28.3 (4.98)	R-24.1 (4.25)	0.041 (0.235)	R-20.8 (3.67)	0.048 (0.272)	0.056 (0.098)
3	R-16.8 (2.96)	R-21.1 (3.72)	R-18.6 (3.28)	0.054 (0.305)	R-17.1 (3.01)	0.059 (0.333)	0.043 (0.074)
	R-24.0 (4.23)	R-28.3 (4.98)	R-24.1 (4.25)	0.041 (0.235)	R-21.5 (3.79)	0.046 (0.264)	0.043 (0.075)

Figure 13. Detail 5.2.33 from Appendix B of the Building Envelope Thermal Bridging Guide (Morrison Hershfield Limited 2020)

A.2 Example Calculation of Linear Transmittance

Example calculation using equations (3) – (5) to find the linear transmittance of an assembly:

The values used in this example calculation are taken from Section 4, Table 7. CMU backup simulation results, heat flux density q (W/m2). The scenario chosen for this example utilizes an HDG proprietary bracket as the stand-off shelf connector, spaced at 610 mm, with 101.6 mm of exterior insulation thickness. The output for this assembly had a heat flux density (q) value of 11.39 W/m^2, and its clear wall counterpart assembly was 7.78 W/m^2. The assembly dimensions are listed in Table 3. Assembly dimensions. The CMU assemblies have an overall height of 2623 mm and a total length of 1200 mm.

The first step is to convert the heat flux density, q (W/m^2) to thermal transmittance per unit area, u (W/m^{2}K):

$$u = \frac{q}{\Delta T} \tag{3}$$

$$u_{full\ wall} = \frac{11.39\ \frac{W}{m^2}}{39\ K} = 0.2921\ \frac{W}{m^2K}$$

And similarly for the clear wall assembly,

$$u_{clear\ wall} = \frac{7.78\ \frac{W}{m^2}}{39\ K} = 0.1995\ \frac{W}{m^2K}$$

Next we calculate the thermal transmittance of a given area, U (W/K):

$$U = u \cdot Area_{wall} \tag{4}$$

$$U_{full\ wall} = 0.2921\ \frac{W}{m^2K} \cdot 2.623\ m \cdot 1.200\ m = 0.9194\ \frac{W}{K}$$

And similarly for the clear wall assembly,

$$U_{clear\ wall} = 0.1995\ \frac{W}{m^2K} \cdot 2.623\ m \cdot 1.200\ m = 0.6279\ \frac{W}{K}$$

Finally we can calculate the linear transmittance, ψ (W/mK):

$$\psi_{full\ wall} = \frac{U_{full\ wall} - U_{clear\ wall}}{L_{wall}} \quad (5)$$

$$\psi_{full\ wall} = \frac{0.9194\ \frac{W}{K} - 0.6279\ \frac{W}{K}}{1.200\ m} = 0.2429\ \frac{W}{m \cdot K}$$

This value coincides with the value presented in Table 8. CMU backup simulation results, linear transmittance ψ (W/mK).

A.3 Additional wood stud at-grade models

The thermal model results in this section follow the same methodology as outlined in **Section 3, Methodology.**

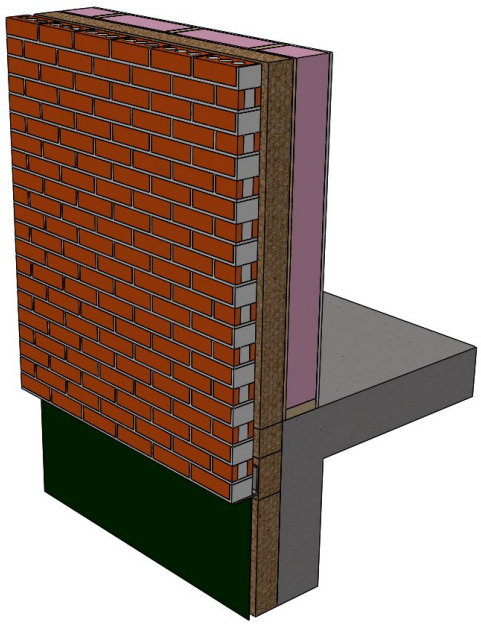

Figure 14. Wood stud assembly at grade

Table 23. Wood stud at grade assembly dimensions

Wood Stud At Grade Dimensions	
Overall Height (mm)	1881
Overall Length (mm)	1200
Concrete Slab Thickness (mm)	203
Concrete Slab Projection[1] (mm)	1000
Total Concrete Wall Height[2] (mm)	703

[1] Perpendicular to the face of the veneer wall, towards the building interior.

[2] Including slab thickness.

Table 24. Wood stud at grade components: dimensions and conductivity

Component	Dimensions (mm)	Conductivity (W/mK)
Interior Film[1]	10 thick	0.083
Gypsum Board	23 thick	0.16
Wood Stud	38 x 140	0.1
Fiberglass Batt Insulation	140	0.042
Exterior Mineral Wool Insulation	50.8 to 101.6 (varies)	0.034
Extruded Polystyrene Insulation	50.8 and 101.6	0.029
Face-Mounted Masonry Ties (Hot-Dip Galvanized)	1.6 thick	62
Intermediate Concrete Slab	203 thick	1.8
Proprietary Bracket	4.76 thick	50
Shelf Angle	101.6 x 101.6, 6.35 thick	50
Vented Air Cavity	25 thick	0.3571
Brick	190 x 57, 90 thick	0.78
Brick Mortar	10 thick	0.5
Exterior Film[1]	10 thick	0.34

[1] Interior and exterior films are needed in order to apply the convective and radiative heat transfer coefficients experienced by the air near the surfaces. It is applied as a layer of thermal resistance.

Table 25. Wood stud at grade backup simulation results, heat flux density q (W/m^2)

Stand-off Shelf Connector	Exterior Insulation Type[1]	Exterior Insulation Thickness (mm)	Intermediate Floor Type (W/mK)	*Heat flux density q (W/m^2)*	
				HDG Connector, 1220 mm spacing	Clear Wall
Proprietary Bracket	XPS	50.8	Concrete (See Figure 14)	12.89	7.02
	Mineral wool	50.8		14.04	7.37
		101.6		8.74	7.47

Table 26. Wood stud at grade backup simulation results, linear transmittance ψ (W/mK)

Stand-off Shelf Connector	**Exterior Insulation Type[1]**	**Exterior Insulation Thickness (mm)**	**Intermediate Floor Type (W/mK)**	***Heat flux density q (W/m²)*** **HDG Connector, 1220 mm spacing**
Proprietary Bracket	XPS	50.8	Concrete (See Figure 14)	0.41
	Mineral wool	50.8		0.46
		101.6		0.09